AN OSCILLATION-FREE DISCONTINUOUS GALERKIN METHOD FOR SCALAR HYPERBOLIC CONSERVATION LAWS

JIANFANG LU[†], YONG LIU[‡], AND CHI-WANG SHU[§]

Abstract. In this paper, we propose a novel discontinuous Galerkin (DG) method to control the spurious oscillations when solving the scalar hyperbolic conservation laws. Usually, the high order linear numerical schemes would generate spurious oscillations when the solution of the hyperbolic conservation laws contains discontinuities. The spurious oscillations maybe harmful to the numerical simulation, as it not only generates some artificial structures not belonging to the problems, but also causes many overshoots and undershoots that make the numerical scheme less robust. To overcome this difficulty, in this paper we introduce a numerical damping term to control spurious oscillations based on the classic DG formulation. Comparing to the classic DG method, the proposed DG method still maintains many good properties, such as the extremely local data structure, conservation, L^2-boundedness, optimal error estimates and superconvergence. We also provide some numerical examples to show the good performance of the proposed DG scheme and verify our theoretical results.

Key words. hyperbolic conservation laws; discontinuous Galerkin; non-oscillatory; optimal error estimates; superconvergence

AMS subject classifications. 65N30, 65N12, 65M60

1. Introduction.

Discontinuous Galerkin methods are a class of finite element methods that have attracted a lot of attention in the last several decades. They have been successfully applied to hyperbolic, elliptic, parabolic and mixed form problems arising from a wide range of applications. Since the DG methods adopt the complete discontinuous basis functions, they have some advantages which are not shared with the typical finite element methods, such as the allowance of arbitrary triangulation with hanging nodes, easy h-p adaptivity, and high parallel efficiency due to the extremely local data structure. The first DG method dates back to 1973, when Reed and Hill solved a steady linear hyperbolic equation in [34]. Later it was coupled with the nonlinearly stable Runge-Kutta time discretization method for solving nonlinear hyperbolic conservation laws by Cockburn et al. in a series of papers [18, 19, 17, 15, 20]. The extension to the convection-diffusion problem and higher order PDEs was carried out in e.g. [5, 21, 41, 12, 40] and the references therein. For more details, we refer to some survey papers [16, 35, 36].

Despite of the excellent performance of the DG methods in dealing with a variety of problems, they become less robust when computing the convection-dominated problems with strong shocks, especially for hyperbolic conservation laws. Due to the nonlinearity of the hyperbolic conservation laws such as inviscid compressible Euler equations, no matter how smooth the initial condition is, the solution can evolve into shock discontinuities at a finite time. This causes numerical difficulty because

[†]South China Research Center for Applied Mathematics and Interdisciplinary Studies, South China Normal University, Canton, Guangdong 510631, China. E-mail: jflu@m.scnu.edu.cn. Research is partially supported by NSFC grant 11901213.

[‡]LSEC, Institute of Computational Mathematics, Hua Loo-Keng Center for Mathematical Sciences, Academy of Mathematics and Systems Science, Chinese Academy of Sciences, Beijing 100190, P.R. China. E-mail: yongliu@lsec.cc.ac.cn. Research is partially supported by the fellowship of China Postdoctoral Science Foundation No. 2020TQ0343.

[§]Division of Applied Mathematics, Brown University, Providence, RI 02912, USA. E-mail: chi-wang_shu@brown.edu. Research is partially supported by NSF grant DMS-2010107 and AFOSR grant FA9550-20-1-0055.

many numerical schemes either cannot correctly compute the shock speed, or generate spurious oscillations near the discontinuity that makes the numerical schemes less robust or even unstable. Through decades, people never stop seeking a way to control spurious oscillations. Among the early works, the first order Godunov scheme [23] possesses monotonicity-preserving property and can resolve the discontinuity monotonically without spurious numerical oscillations. However, Godunov pointed out that if a numerical scheme preserves the monotonicity then it is at most first order accurate. This result is somehow frustrating and could prevent people from attempting to improve the Godunov scheme. This also explains the numerical solution is often smeared too much near the discontinuity for the relatively large built-in numerical dissipation in the Godunov scheme. Fortunately, there is an assumption in Godunov's proof that the numerical scheme is linear when solving a linear advection equation. By realizing the Godunov's theorem could be circumvented, the so-called high-resolution schemes were devised in 1970s and 1980s, such as MUSCL schemes [38], TVD schemes [25], and PPM schemes [22], etc. These high resolution schemes are usually second order accurate in smooth region, and can resolve the discontinuity monotonically with a sharper transition than first order schemes. They are popular in applications for the balance between computational cost and desired resolution, especially for problems with shocks and other discontinuities and relatively simple structures between these discontinuities. For problems containing both shocks and complicated smooth structures, such as the shock interaction with vortices or acoustic waves, the higher order schemes in an essentially non-oscillatory (ENO) fashion are favorable [26, 37, 28]. Such high order ENO schemes can be constructed up to arbitrary order of accuracy, and produce sharp and ENO shock transitions even for strong shocks, which also explains their rapid popularity and widespread applications as soon as they were born.

To control spurious oscillations near the discontinuity for the DG methods, different kinds of limiters were developed such as the *minmod*-type total variation diminishing (TVD) limiter, total variation bounded (TVB) limiter and weighted essentially non-oscillatory (WENO) limiter, etc. For more details, see e.g. [35, 33, 44] and references therein. The mechanism of limiters is to modify the numerical solution after we have obtained it, with various tools and indicators to determine whether the numerical solution is "bad" or not within a cell and to perform a limiting process once the "bad" cell is marked. Sometimes the limiter is problem-dependent, and it may destroy some good properties of the original schemes. Another approach is to introduce artificial terms, such as artificial diffusion, directly in the weak formulation so as to obtain certain properties such as entropy stability or shock capturing, see e.g. [27]. However, the artificial diffusion usually involves parameters, which might be problem dependent, and if these parameters are not adjusted properly, the numerical solution either could have too much smearing for shocks, or the spurious oscillations could still be visible and cannot be negligible. The advantage of the artificial diffusion approach is that it is embedded in the weak formulation, which facilitates theoretical analysis and certain applications such as steady state computation. In this paper, we propose a different approach to control spurious oscillations in the DG methods for solving scalar hyperbolic conservation laws. Based on the conventional DG scheme, we introduce a damping term in it to control the high order terms. The added damping term is similar in spirit to the so-called "local projection stabilization" schemes, please see [2, 3] and references therein. Similar idea of this projection-based operator has also been used in the virtual element methods [4]. By a unified choice of the damp-

ing coefficients, the damping term would be small when the numerical solution stays smooth, and takes effect near the discontinuity. To be more specific, this approach can automatically detect the intensity of the discontinuity and control the numerical oscillation near the strong discontinuity without any problem-dependent parameters. Theoretical analysis shows that the proposed DG scheme maintains many good properties such as conservation, L^2-boundedness, and optimal error estimates, etc. For one-dimensional linear scalar conservation laws, we also study the superconvergence behavior using the correction function technique [11]. For two-dimensional problems, we prove the optimal error estimates with P^k-elements by using the shifting technique [31]. Numerical evidences verify all the theoretical results, and the numerical solution does behave non-oscillatory around the discontinuity indicating that the proposed DG method controls spurious numerical oscillations effectively.

This paper is organized as follows. In Section 2, we propose a novel DG scheme for solving one-dimensional scalar conservation laws. Then we show the proposed DG scheme is conservative, L^2-bounded, and has an optimal error estimation. Moreover, with the correction function technique [11], we study the superconvergence of the proposed DG method. In Section 3, we extend the algorithm to the multidimensional scalar conservation laws. We also show the proposed DG scheme is conservative, L^2-bounded, and has an optimal error estimation on the uniform Cartesian meshes using P^k-elements. In Section 4, we show several numerical examples including both the linear and nonlinear scalar problems in one and two dimensions. Concluding remarks are given in Section 5.

2. One-dimensional scalar conservation laws. In this section, we propose a new DG scheme for solving the one-dimensional hyperbolic conservation laws. As we shall see later, the proposed DG scheme is based on the classic DG methods, with an extra damping term in it. It not only possesses the property of conservation, but also maintains the L^2-boundedness, the optimal error estimates and superconvergence result analogous to the classic DG schemes.

2.1. Scheme formulation. In this subsection, we first take a brief review of the classic DG method for solving the one-dimensional scalar conservation laws in the following

$$\begin{cases} u_t + f(u)_x = 0, & (x,t) \in (a,b) \times (0,T], \\ u(x,0) = u_0(x), & x \in (a,b) \end{cases} \tag{2.1}$$

with periodic or compactly supported boundary conditions. Throughout this paper, we consider the problems with the periodic or the compactly supported boundary conditions only, while it can be generalized to problems with inflow boundary conditions without any difficulty.

Take partition of (a,b) into N cells, and we then have

$$a = x_{\frac{1}{2}} < x_{\frac{3}{2}} < \cdots < x_{N+\frac{1}{2}} = b,\ h_j = x_{j+\frac{1}{2}} - x_{j-\frac{1}{2}},\ I_j = \left(x_{j-\frac{1}{2}}, x_{j+\frac{1}{2}}\right). \tag{2.2}$$

We also assume that the mesh is quasi-uniform, i.e. there exists a constant $\nu > 0$ such that

$$h \le \nu\, \rho, \quad h = \max_j h_j,\ \rho = \min_j h_j\,. \tag{2.3}$$

The standard semi-discrete DG scheme is as follows: Find $u_h^c(\cdot,t) \in V_h^k$ such that

$$\int_{I_j} (u_h^c)_t v_h\, dx = \int_{I_j} f(u_h^c)(v_h)_x\, dx - \hat{f}_{j+\frac{1}{2}}(v_h)^-_{j+\frac{1}{2}} + \hat{f}_{j-\frac{1}{2}}(v_h)^+_{j-\frac{1}{2}},\ \forall\, v_h \in V_h^k\,, \tag{2.4}$$

where $(v_h)^{\pm}_{j+\frac{1}{2}} = v_h\big(x^{\pm}_{j+\frac{1}{2}}\big)$ and $\hat{f}_{j+\frac{1}{2}}$ is the monotone flux, such as the Godunov flux or the Lax-Friedrichs flux, etc. The finite element space V_h^k is defined as follows

$$V_h^k := \big\{ v \in L^2([a,b]) : v|_{I_j} \in P^k(I_j), \quad j = 1, \ldots, N \big\}, \tag{2.5}$$

where $P^k(I_j)$ denotes the set of all polynomials of degree not greater than k on I_j. It is widely known that the DG scheme (2.4) possesses many good properties and we present them as follows. When $v_h = 1$ in (2.4) and sum it over j, we have the conservation given by

$$\frac{d}{dt}\int_a^b u_h^c(x,t)\,dx = 0\,. \tag{2.6}$$

Also, take $v_h = u_h^c$ in (2.4) and sum it over j, then we obtain the L^2-stability of the scheme (2.4):

$$\frac{1}{2}\frac{d}{dt}\int_a^b (u_h^c)^2\,dx = -\sum_j \Theta_{j+\frac{1}{2}}\,, \tag{2.7}$$

where $\Theta_{j+\frac{1}{2}}$ is defined as

$$\Theta_{j+\frac{1}{2}} = \int_{(u_h^c)^-_{j+\frac{1}{2}}}^{(u_h^c)^+_{j+\frac{1}{2}}} \Big(f(y) - \hat{f}\big((u_h^c)^-_{j+\frac{1}{2}}, (u_h^c)^+_{j+\frac{1}{2}}\big)\Big)\,dy \geq 0\,. \tag{2.8}$$

For the linear case $f(u) = au$, a is a constant and the upwind numerical fluxes are adopted in (2.4). If the exact solution stays smooth, we then have the following optimal error estimates:

$$\|u(\cdot,t) - u_h^c(\cdot,t)\| \lesssim h^{k+1}\,, \tag{2.9}$$

where $\|\cdot\|$ is the standard L^2 norm on (a,b), and $A \lesssim B$ means that there exists a constant $c_0 > 0$ independent of h such that $A \leq c_0 B$. For more details, we refer the readers to e.g. [35] and the references therein. Furthermore, the authors in [12, 11] obtained the superconvergence result between the projection of the exact solution and the numerical solution for the DG scheme (2.4). With these good properties, the DG scheme (2.4) works very well in computing the hyperbolic conservation laws. It not only maintains high order accuracy in the smooth region, but also captures discontinuities (especially weak discontinuities) well. However, it generates some spurious oscillations near the discontinuity, which makes the scheme less robust. To overcome this difficulty, many limiters have been developed to control spurious oscillations, such as the *minmod* type total variation diminishing (TVD) limiter, total variation bounded (TVB) limiter and weighted essentially non-oscillatory (WENO) limiter, etc. See [35, 44] and the references therein. Now we proceed to construct a DG scheme for solving (2.1) that possesses the above good properties, and also controls spurious oscillations automatically. The new DG scheme is defined as follows: Find $u_h(\cdot,t) \in V_h^k$ such that

$$\begin{aligned}\int_{I_j} (u_h)_t v_h\,dx = \int_{I_j} f(u_h)(v_h)_x\,dx - \hat{f}_{j+\frac{1}{2}}(v_h)^-_{j+\frac{1}{2}} + \hat{f}_{j-\frac{1}{2}}(v_h)^+_{j-\frac{1}{2}} \\ - \sum_{l=0}^{k} \frac{\sigma_j^l}{h_j}\int_{I_j} \big(u_h - P_h^{l-1}u_h\big)v_h\,dx, \quad \forall\, v_h \in V_h^k\,,\end{aligned} \tag{2.10}$$

where P_h^l, $l \geq 0$, is the standard L^2 projection into V_h^l, that is, for any function w, $P_h^l w \in V_h^l$ satisfies

$$\int_{I_j} (P_h^l w - w) v_h \, dx = 0, \quad \forall \, v_h \in \mathbb{P}^l(I_j) \, . \tag{2.11}$$

We also define $P_h^{-1} = P_h^0$. Particularly, $P_h^0 w = (\overline{w})_j$ on I_j, where $(\overline{w})_j$ denotes the cell average of w on I_j. $\sigma_j^l \geq 0$ has to be chosen carefully so that they are small in smooth region, and becomes large near discontinuities. In this paper, they are taken as follows.

$$\sigma_j^l = \frac{2\,(2l+1)}{(2k-1)} \frac{h^l}{l!} \Big([\![\partial_x^l u_h]\!]^2_{j+\frac{1}{2}} + [\![\partial_x^l u_h]\!]^2_{j-\frac{1}{2}} \Big)^{\frac{1}{2}}, \quad k \geq 1, \tag{2.12}$$

where $[\![v]\!]_{j+\frac{1}{2}} = v\big(x^+_{j+\frac{1}{2}}\big) - v\big(x^-_{j+\frac{1}{2}}\big)$ denotes the jump of v at $x = x_{j+\frac{1}{2}}$.

REMARK 2.1. *It is widely known the first order monotone scheme possesses many good properties such as TVD, monotonicity-preserving, and convergent to the entropy solution, etc. Intuitively, the mechanism of controlling the spurious oscillations can be explained as follows. As the damping coefficients in* (2.12) *are large, the high frequency waves are damped out as time evolves, then the DG scheme* (2.10) *behaves as the first order scheme near the discontinuity.*

2.2. Conservation, L^2-boundedness and optimal error estimates.

2.2.1. Conservation. Take $v_h = 1$ in (2.10), we have

$$\begin{aligned} \frac{d}{dt} \int_{I_j} u_h \, dx &= - \hat{f}_{j+\frac{1}{2}} + \hat{f}_{j-\frac{1}{2}} - \sum_{l=0}^{k} \frac{\sigma_j^l}{h_j} \int_{I_j} \big(u_h - P_h^{l-1} u_h \big) \, dx \\ &= - \hat{f}_{j+\frac{1}{2}} + \hat{f}_{j-\frac{1}{2}} \, . \end{aligned}$$

Sum it over j, with the periodic or the compactly supported boundary conditions, and we obtain the conservation result similar to (2.6).

2.2.2. L^2-boundedness. Take $v_h = u_h$ in (2.10) and sum it over j, and we have

$$\begin{aligned} \frac{1}{2} \frac{d}{dt} \int_a^b (u_h)^2 \, dx &= - \sum_j \Theta_{j+\frac{1}{2}} - \sum_j \sum_{l=0}^{k} \frac{\sigma_j^l}{h_j} \int_{I_j} \big(u_h - P_h^{l-1} u_h \big) u_h \, dx \\ &= - \sum_j \Theta_{j+\frac{1}{2}} - \sum_j \sum_{l=0}^{k} \frac{\sigma_j^l}{h_j} \int_{I_j} \big(u_h - P_h^{l-1} u_h \big)^2 \, dx \leq 0 \, , \end{aligned}$$

where $\Theta_{j+\frac{1}{2}}$ is defined in (2.8). Then we obtain $\|u_h(\cdot,t)\| \leq \|u_h(\cdot,0)\|$.

2.2.3. A priori error estimates. We present the a priori error estimates for the linear scalar conservation laws with $f(u) = au$. Without loss of generality, we assume $a = 1$. We take the upwind fluxes $\hat{f}_{j+\frac{1}{2}} = (u_h)^-_{j+\frac{1}{2}}$ in (2.10). For the classic DG method, the optimal error estimate is obtained thanks to the Gauss-Radau projection [35]. While in our method, there is an extra damping term that needs to be estimated. We now introduce some inverse inequalities [14] as follows: For $w_h \in V_h^k$, there exists a positive constant C independent of w_h and h such that

$$\|\partial_x w_h\| \leq C h^{-1} \|w_h\|; \quad \|w_h\|_{L^\infty} \leq C h^{-1/2} \|w_h\|. \tag{2.13}$$

We now proceed to obtain the error estimate of the numerical solution generated by the semi-discrete DG scheme (2.10), stated in the following theorem.

THEOREM 2.1. *For any given integer $k \geq 1$, suppose $u(\cdot,t) \in H^{k+1}([a,b])$ is the exact solution of the problem* (2.1) *with the linear flux $f(u) = u$ and u_h is the numerical solution of DG scheme* (2.10)*. The initial data is chosen by $u_h(x,0) = P_h^k u_0$, where P_h^k is the standard L^2 projection defined in* (2.11)*, then we have*

$$\left\|u(\cdot,t) - u_h(\cdot,t)\right\| \lesssim h^{k+1}\,. \tag{2.14}$$

For the exact solution u to (2.1), we have

$$\int_{I_j} u_t v_h\,dx + B_j(u,v_h) = 0, \quad \forall\, v_h \in V_h^k\,, \tag{2.15}$$

where B_j is defined as

$$B_j(w,v_h) = -\int_{I_j} w\,(v_h)_x\,dx + w^-_{j+\frac{1}{2}}(v_h)^-_{j+\frac{1}{2}} - w^-_{j-\frac{1}{2}}(v_h)^+_{j-\frac{1}{2}}\,. \tag{2.16}$$

Subtracting (2.10) from (2.15), we have

$$\int_{I_j} e_t v_h\,dx + B_j(e,v_h) = \sum_{l=0}^{k} \frac{\sigma_j^l}{h_j} \int_{I_j} \big(u_h - P_h^{l-1}u_h\big) v_h\,dx\,, \quad \forall\, v_h \in V_h^k\,, \tag{2.17}$$

where $e = u - u_h$. Denote $e = \xi - \eta$, $\xi = P_h^- u - u_h$, $\eta = P_h^- u - u$, and P_h^- is the Gauss-Radau projection defined as follows. For any function w, $P_h^- w \in V_h^k$ such that

$$\begin{cases} \displaystyle\int_{I_j} (P_h^- w - w) v_h\,dx = 0, \quad \forall\, v_h \in P^{k-1}(I_j), \\ P_h^- w(x^-_{j+\frac{1}{2}}) = w(x_{j+\frac{1}{2}}). \end{cases} \tag{2.18}$$

If the function $w \in H^{k+1}([a,b])$, then we have the following approximation properties

$$h^l \|\partial_x^l (P_h^- w - w)\| + h^{l+\frac{1}{2}} \|\partial_x^l (P_h^- w - w)\|_{L^2(\Gamma_h)} \lesssim h^{k+1}, \quad l = 0,\ldots,k, \tag{2.19}$$

where $\|w\|_{L^2(\Gamma_h)} := \Big(\sum_j \Big(\big(w^+_{j+\frac{1}{2}}\big)^2 + \big(w^-_{j+\frac{1}{2}}\big)^2\Big)\Big)^{\frac{1}{2}}$. Then for $\forall\, v_h \in V_h^k$, the error equation (2.17) becomes

$$\begin{aligned} &\int_{I_j} \xi_t v_h\,dx + B_j(\xi,v_h) + \sum_{l=0}^{k} \frac{\sigma_j^l}{h_j} \int_{I_j} \big(\xi - P_h^{l-1}\xi\big) v_h\,dx \\ &\quad = \int_{I_j} \eta_t v_h\,dx + B_j(\eta,v_h) + \sum_{l=0}^{k} \frac{\sigma_j^l}{h_j} \int_{I_j} \Big(P_h^- u - P_h^{l-1}\big(P_h^- u\big)\Big) v_h\,dx\,. \end{aligned} \tag{2.20}$$

With the definition of the projection P_h^- we have $B_j(\eta,v_h) = 0$. Taking $v_h = \xi$ in (2.20) and summing it over j, we then have

$$\frac{1}{2}\frac{d}{dt}\int_a^b \xi^2\,dx + \frac{1}{2}\sum_j [\![\xi]\!]^2_{j+\frac{1}{2}} + \sum_j \sum_{l=0}^{k} \frac{\sigma_j^l}{h_j} \int_{I_j} \big(\xi - P_h^{l-1}\xi\big)^2\,dx = A_1 + A_2\,, \tag{2.21}$$

where A_1, A_2 are given as

$$A_1 = \sum_j \int_{I_j} \eta_t \xi \, dx, \quad A_2 = \sum_j \sum_{l=0}^{k} \frac{\sigma_j^l}{h_j} \int_{I_j} \Big(P_h^- u - P_h^{l-1}(P_h^- u) \Big) \xi \, dx \,.$$

For A_1, we have

$$|A_1| \lesssim h^{k+1} \|\xi\| \,. \tag{2.22}$$

For A_2, on I_j we have

$$\begin{aligned} &\big\| P_h^- u - P_h^{l-1}(P_h^- u) \big\|_{L^2(I_j)} \\ &\quad \le \big\| P_h^- u - u \big\|_{L^2(I_j)} + \big\| u - P_h^{l-1} u \big\|_{L^2(I_j)} + \big\| P_h^{l-1}(u - P_h^- u) \big\|_{L^2(I_j)} \\ &\quad \lesssim h^{\max(1,l)+\frac{1}{2}}, \quad l = 0, \ldots, k. \end{aligned} \tag{2.23}$$

and with the definition of σ_j^l in (2.12) we have

$$\begin{aligned} (\sigma_j^l)^2 &= \frac{4\,(2l+1)^2}{(2k-1)^2} \frac{h^{2l}}{(l!)^2} \Big([\![\partial_x^l (u_h - u)]\!]_{j-\frac{1}{2}}^2 + [\![\partial_x^l (u_h - u)]\!]_{j+\frac{1}{2}}^2 \Big) \\ &\lesssim h^{2l} \Big([\![\partial_x^l \xi]\!]_{j-\frac{1}{2}}^2 + [\![\partial_x^l \xi]\!]_{j+\frac{1}{2}}^2 \Big) + h^{2l} \Big([\![\partial_x^l \eta]\!]_{j-\frac{1}{2}}^2 + [\![\partial_x^l \eta]\!]_{j+\frac{1}{2}}^2 \Big) \,. \end{aligned} \tag{2.24}$$

By Cauchy-Schwarz inequality and inverse inequality (2.13), (2.23) and (2.24), we then have

$$\begin{aligned} A_2 &\le \sum_j \sum_{l=0}^{k} \frac{\sigma_j^l}{h_j} \big\| P_h^- u - P_h^{l-1}(P_h^- u) \big\|_{L^2(I_j)} \|\xi\|_{L^2(I_j)} \\ &\lesssim \sum_j \sum_{l=0}^{k} h^{\max\left(l-\frac{1}{2},\frac{1}{2}\right)+l} \Big([\![\partial_x^l \xi]\!]_{j-\frac{1}{2}}^2 + [\![\partial_x^l \xi]\!]_{j+\frac{1}{2}}^2 \Big)^{\frac{1}{2}} \|\xi\|_{L^2(I_j)} \\ &\qquad + \sum_j \sum_{l=0}^{k} h^{\max\left(l-\frac{1}{2},\frac{1}{2}\right)+l} \Big(\Big([\![\partial_x^l \eta]\!]_{j-\frac{1}{2}}^2 + [\![\partial_x^l \eta]\!]_{j+\frac{1}{2}}^2 \Big)^{\frac{1}{2}} \Big) \|\xi\|_{L^2(I_j)} \\ &\lesssim \Big(\sum_j \sum_{l=0}^{k} h^{2l} [\![\partial_x^l \xi]\!]_{j+\frac{1}{2}}^2 \Big)^{\frac{1}{2}} h^{\frac{1}{2}} \|\xi\| + \Big(\sum_j \sum_{l=0}^{k} h^{2l} [\![\partial_x^l \eta]\!]_{j+\frac{1}{2}}^2 \Big)^{\frac{1}{2}} h^{\frac{1}{2}} \|\xi\| \\ &\lesssim \|\xi\|^2 + h^{2k+2} \,. \end{aligned} \tag{2.25}$$

In the last inequality of (2.25) we have used the following facts by (2.13) and (2.19)

$$\begin{aligned} \sum_j \sum_{l=0}^{k} h^{2l} [\![\partial_x^l \xi]\!]_{j+\frac{1}{2}}^2 &\lesssim \sum_j \sum_{l=0}^{k} h^{2l} \Big(\Big((\partial_x^l \xi)_{j+\frac{1}{2}}^+ \Big)^2 + \Big((\partial_x^l \xi)_{j+\frac{1}{2}}^- \Big)^2 \Big) \\ &\lesssim h^{-1} \sum_{l=0}^{k} h^{2l} \|\partial_x^l \xi\|^2 \lesssim h^{-1} \|\xi\|^2 \,, \\ \sum_j \sum_{l=0}^{k} h^{2l} [\![\partial_x^l \eta]\!]_{j+\frac{1}{2}}^2 &\lesssim \sum_j \sum_{l=0}^{k} h^{2l} \Big(\Big((\partial_x^l \eta)_{j+\frac{1}{2}}^+ \Big)^2 + \Big((\partial_x^l \eta)_{j+\frac{1}{2}}^- \Big)^2 \Big) \lesssim h^{2k+1} \,. \end{aligned} \tag{2.26}$$

Now we plug (2.22) and (2.25) into (2.20), and obtain

$$\frac{1}{2}\frac{d}{dt}\int_a^b \xi^2\,dx + \frac{1}{2}\sum_j [\![\xi]\!]^2_{j+\frac{1}{2}} + \sum_j \sum_{l=0}^{k} \frac{\sigma_j^l}{h_j}\int_{I_j} \left(\xi - P_h^{l-1}\xi\right)^2 dx \lesssim \|\xi\|^2 + h^{2k+2}\,. \tag{2.27}$$

With the Grönwall's inequality, namely supposing $\frac{d}{dt}y(t) \le ay(t) + b(t)$, then we have

$$y(t) \le e^{at}y(0) + \int_0^t e^{a(t-r)}b(r)\,dr, \tag{2.28}$$

we can obtain $\|\xi(\cdot,t)\| \lesssim \|\xi(\cdot,0)\| + h^{k+1}$. We could take the standard L^2 projection of the initial condition such that $\|\xi(\cdot,0)\| \lesssim h^{k+1}$, together with the approximation properties (2.19), to obtain the error estimates $\|e\| \le \|\xi\| + \|\eta\| \lesssim h^{k+1}$.

2.3. Superconvergence. In the past few years, there has been considerable interest in studying the superconvergence properties of the DG methods. We refer to [13] for one-dimensional hyperbolic conservation laws and time-dependent convection-diffusion equations, for which the authors obtained the $(k+1/2)$-th superconvergence rate between the numerical solution and the Gauss-Radau projection of the exact solution by taking special test functions. Later, Yang and Shu in [42] obtained a $(k+2)$-th superconvergence rate of the DG approximation at the right Radau points when upwind fluxes were used. In 2014, Cao et al. [11] introduced an approach to study the superconvergence of the DG methods for linear hyperbolic equations. They constructed a suitable correction function to correct the error between the exact solution and its special projection to obtain the optimal $(2k+1)$-th superconvergence rate at the downwind points. Later, this technique is developed to study other kinds of DG methods, such as the local DG method, the direct DG method, the energy-conserving DG method and the ultra-weak local DG method, etc. [7, 8, 9, 6, 10, 30, 32]. For other superconvergence results of DG methods in 2D or 3D, we refer to [1, 39]. Superconvergence results are foundations of designing trouble cell indicators such as the KXRCF trouble cell indicator [29], which is a key point for adaptive DG schemes. Thus, we are also very interested in studying the superconvergence properties of the newly proposed DG method. Now we continue to derive a superconvergence result for the DG scheme (2.10), stated in the following theorem.

THEOREM 2.2. *For any given integer $k \ge 1$, suppose $u(\cdot,t) \in H^{k+3}([a,b])$ is the exact solution of the problem (2.1) with the linear flux $f(u) = u$ and u_h is the numerical solution of DG scheme (2.10). The initial data is chosen by $u_h(x,0) = P_h^- u_0$, then we have*

$$\left\|u_h - P_h^- u\right\| \lesssim h^{k+2}. \tag{2.29}$$

To obtain the above superconvergence of the DG scheme, we firstly need to estimate ξ_t. Indeed, we have the following lemma.

LEMMA 2.1. *For the DG scheme (2.10), we have the error estimate of ξ_t that*

$$\|\xi_t(\cdot,t)\| \lesssim h^{k+1}. \tag{2.30}$$

The proof of Lemma 2.1 is given in the Appendix; see Section 6.1.

In light of the error estimate of ξ, with (2.24) and (2.26) we then have

$$\Big(\sum_j \sum_{l=0}^{k} |\sigma_j^l|^2\Big)^{\frac{1}{2}} \lesssim h^{k+\frac{1}{2}}. \tag{2.31}$$

In the proof of Lemma 2.1 in the Appendix, we also have the estimate for $\big(\sigma_j^l\big)_t$. A similar derivation gives us the following estimation from (6.5) and (2.30).

$$\Big(\sum_j \sum_{l=0}^{k} |(\sigma_j^l)_t|^2\Big)^{\frac{1}{2}} \lesssim h^{k+\frac{1}{2}}. \tag{2.32}$$

Next we define the correction function to improve the estimate for ξ: For any j, find the correction function $w \in P^k(I_j)$ such that

$$\begin{cases} \displaystyle\int_{I_j} w\,(v_h)_x\,dx = L(v_h)_j, \quad \forall\, v_h \in P^k(I_j), \\ w^-_{j+\frac{1}{2}} = 0\,, \end{cases} \tag{2.33}$$

where $L(v_h)_j$ is given as

$$L(v_h)_j = \int_{I_j} \eta_t v_h\,dx + \sum_{l=0}^{k} \frac{\sigma_j^l}{h_j} \int_{I_j} \Big(P_h^- u - P_h^{l-1}\big(P_h^- u\big)\Big) v_h\,dx\,.$$

Then from the definition of $B_j(\cdot,\cdot)$ in (2.16), we obtain $B_j(w, v_h) = -L(v_h)_j$. By (2.19) and Cauchy-Schwarz inequality, we have

$$\big|L(v_h)_j\big| \lesssim \|\eta_t\|_{L^2(I_j)} \|v_h\|_{L^2(I_j)} + h^{\frac{1}{2}} \left(\sum_{l=0}^{k} \big|\sigma_j^l\big|^2\right)^{\frac{1}{2}} \|v_h\|_{L^2(I_j)}. \tag{2.34}$$

Thus, for the correction function w we have the following estimation.

Lemma 2.2. *The correction function w is well defined by* (2.33) *and has the following estimation*

$$\begin{aligned} \|w\|_{L^2(I_j)} &\lesssim h\,\|\eta_t\|_{L^2(I_j)} + h^{\frac{3}{2}} \left(\sum_{l=0}^{k} |\sigma_j^l|^2\right)^{\frac{1}{2}}, \\ \|w_t\|_{L^2(I_j)} &\lesssim h\,\|\eta_{tt}\|_{L^2(I_j)} + h^{\frac{3}{2}} \left(\sum_{l=0}^{k} \big|\sigma_j^l\big|^2\right)^{\frac{1}{2}} + h^{\frac{3}{2}} \left(\sum_{l=0}^{k} \big|(\sigma_j^l)_t\big|^2\right)^{\frac{1}{2}}. \end{aligned} \tag{2.35}$$

The proof of Lemma 2.2 is given in the Appendix; see Section 6.2.

Therefore, with the aid of the correction function w, we are able to improve the convergence order in the estimate of ξ. We add the function w to both sides of the error equation (2.20) and obtain

$$\begin{aligned} &\int_{I_j} (\xi + w)_t v_h\,dx + B_j(\xi + w, v_h) + \sum_{l=0}^{k} \frac{\sigma_j^l}{h_j} \int_{I_j} \big(\xi + w - P_h^{l-1}(\xi + w)\big) v_h\,dx \\ &= \int_{I_j} (w)_t v_h\,dx + B_j(w, v_h) + \sum_{l=0}^{k} \frac{\sigma_j^l}{h_j} \int_{I_j} \big(w - P_h^{l-1} w\big) v_h\,dx \end{aligned}$$

$$
\begin{aligned}
&+\int_{I_j}\eta_t v_h\,dx+\sum_{l=0}^{k}\frac{\sigma_j^l}{h_j}\int_{I_j}\Big(P_h^- u-P_h^{l-1}\big(P_h^- u\big)\Big)v_h\,dx\\
&=\int_{I_j}(w)_t v_h\,dx-\int_{I_j}w(v_h)_x\,dx+\sum_{l=0}^{k}\frac{\sigma_j^l}{h_j}\int_{I_j}\big(w-P_h^{l-1}w\big)v_h\,dx\\
&\quad+\int_{I_j}\eta_t v_h\,dx+\sum_{l=0}^{k}\frac{\sigma_j^l}{h_j}\int_{I_j}\Big(P_h^- u-P_h^{l-1}\big(P_h^- u\big)\Big)v_h\,dx\\
&=\int_{I_j}(w)_t v_h\,dx+\sum_{l=0}^{k}\frac{\sigma_j^l}{h_j}\int_{I_j}\big(w-P_h^{l-1}w\big)v_h\,dx\\
&\lesssim\left(h\,\|\eta_{tt}\|_{L^2(I_j)}+h^{\frac{3}{2}}\Big(\sum_{l=0}^{k}\big|\sigma_j^l\big|^2\Big)^{\frac{1}{2}}+h^{\frac{3}{2}}\Big(\sum_{l=0}^{k}\big|(\sigma_j^l)_t\big|^2\Big)^{\frac{1}{2}}\right)\|v_h\|_{L^2(I_j)}\\
&\quad+h^{\frac{3}{2}}\Big(\sum_{l=0}^{k}\big|\sigma_j^l\big|^2\Big)^{\frac{1}{2}}\|v_h\|_{L^2(I_j)}\,.
\end{aligned}
\tag{2.36}
$$

Here we have used the definition of the correction function w (2.33) in the second and third equalities in (2.36). Take $v_h=\xi+w$ in (2.36), by the stability analysis and Cauchy-Schwarz inequality, we obtain

$$
\begin{aligned}
&\frac{1}{2}\frac{d}{dt}\|\xi+w\|^2\\
&\lesssim\left(h\|\eta_{tt}\|+h^{\frac{3}{2}}\Big(\sum_j\sum_{l=0}^{k}\big|\sigma_j^l\big|^2\Big)^{\frac{1}{2}}+h^{\frac{3}{2}}\Big(\sum_j\sum_{l=0}^{k}\big|(\sigma_j^l)_t\big|^2\Big)^{\frac{1}{2}}\right)\|\xi+w\|\,.
\end{aligned}
\tag{2.37}
$$

This, together with (2.31) and (2.32), leads to

$$
\frac{d}{dt}\|\xi+w\|\lesssim h^{k+2}.
\tag{2.38}
$$

Thus, we have

$$
\|\xi\|\le\|\xi+w\|+\|w\|\lesssim h^{k+2}\,.
\tag{2.39}
$$

Therefore, we obtain $(k+2)$-th order superconvergence result.

As a direct consequence of Theorem 2.2, we have the following superconvergence results of the fluxes, the cell averages and errors at Gauss-Radau points, respectively.

COROLLARY 2.1. *For any given integer $k\ge1$, suppose $u(\cdot,t)\in H^{k+3}([a,b])$ is the the exact solution of the problem* (2.1) *for the linear case $f(u)=u$ and u_h is the approximation of the DG scheme* (2.10). *The initial discretization is chosen by $u_h(x,0)=P_h^- u_0$, then we have*

$$
e_{u,c}\lesssim h^{k+2},\quad e_{u,f}\lesssim h^{k+2},\quad e_{u,p}\lesssim h^{k+\frac{3}{2}}.
\tag{2.40}
$$

where $e_{u,c},e_{u,f}$ and $e_{u,p}$ are given as

$$
\begin{aligned}
&e_{u,c}:=\left(\frac{1}{N}\sum_j\Big(\frac{1}{h_j}\int_{I_j}(u-u_h)\,dx\Big)^2\right)^{\frac{1}{2}};\\
&e_{u,f}:=\left(\frac{1}{N}\sum_j\big(u_{j+\frac{1}{2}}-(u_h)^-_{j+\frac{1}{2}}\big)^2\right)^{\frac{1}{2}};\ e_{u,p}:=\max_{j,\ell}\big|(u-u_h)(G_{j,\ell})\big|\,,
\end{aligned}
\tag{2.41}
$$

where $G_{j,\ell}$ are the right Gauss-Radau points on the subinterval I_j. We provide the proof of Corollary 2.1 in the Appendix; see Section 6.3.

REMARK 2.2. *In [43], the authors developed a maximum-principle-satisfying limiter for the finite volume methods and the discontinuous Galerkin methods, which solved the hyperbolic conservation laws successfully. The essence of the limiter is to keep the cell averages of the numerical solution within the range. As long as the cell averages stay in the range, a compression technique is performed to the numerical solution such that all quadrature points are confined in that range. Since the high order approximation for the cell averages can be written as a convex combination of several first order monotone schemes, the cell averages would stay in the range under a suitable CFL condition in one step Euler forward. We remark that the new DG scheme* (2.10) *is compatible with the maximum-principle-satisfying limiter, and the damping term does not bring any troubles when applying the limiter to the schemes.*

REMARK 2.3. *In [11], the authors obtained the optimal $(2k+1)$-th superconvergence rates for numerical fluxes and cell averages. Since the Gauss-Radau projection is orthogonal to the polynomials of degree $k-1$, the authors then constructed k correction functions to improve the errors between the numerical solution and the Gauss-Radau projection of the exact solution up to $(2k+1)$-th order. However, in our method the additional term vanishes only for $v_h = 1$, thus the correction function w defined in* (2.33) *has no more orthogonality. Therefore, we can only obtain $(k+2)$-th superconvergence rate and numerical examples also confirm that our theoretical analysis is sharp, please see Section 4.*

3. Multidimensional scalar problems. In this section, we extend the one-dimensional DG scheme (2.10) to the scalar hyperbolic conservation laws in multidimensions. We also show that the proposed DG scheme is conservative, L^2-bounded, and has an optimal error estimation using P^k-elements.

3.1. Scheme formulation. The governing equation is given as follows

$$\begin{cases} u_t + \nabla \cdot \boldsymbol{f}(u) = 0, & (\boldsymbol{x}, t) \in \Omega \times (0, T], \\ u(\boldsymbol{x}, 0) = u_0(\boldsymbol{x}), & \boldsymbol{x} \in \Omega \end{cases} \tag{3.1}$$

with periodic or compactly supported boundary conditions. The domain Ω is bounded in $\mathbb{R}^d$ and $\boldsymbol{x} = (x_1, \ldots, x_d) \in \mathbb{R}^d$. Assume we have the partition $\mathcal{T}_h$ of Ω and $\mathcal{T}_h$ is regular. We still adopt the notations similar as in Section 2 without causing any ambiguities.

$$h = \max_{K \in \mathcal{T}_h} h_K, \ h_K = \text{ diam } K, \ \rho = \min_{K \in \mathcal{T}_h} \rho_K,$$

ρ_K is the diameter of the sphere inscribed in K. The DG scheme for (3.1) is presented as follows: Find $u_h(\cdot, t) \in V_h^k$ such that

$$\begin{aligned} \int_K (u_h)_t v_h \, d\boldsymbol{x} = & \int_K \boldsymbol{f}(u_h) \cdot \nabla v_h \, d\boldsymbol{x} + \int_{\partial K} \widehat{\boldsymbol{f}}(u_h) \cdot \boldsymbol{n}_K v_h \, dS \\ & - \sum_{l=0}^{k} \frac{\sigma_K^l}{h_K} \int_K \big(u_h - P_h^{l-1} u_h\big) v_h \, d\boldsymbol{x}, \quad \forall \, v_h \in V_h^k \,, \end{aligned} \tag{3.2}$$

where $\widehat{\boldsymbol{f}}(u_h)$ is taken as the monotone flux on the element interfaces, and $\boldsymbol{n}_K$ is the outward unit normal respect to ∂K. V_h^k is the finite element space containing

piecewise polynomials of degree not greater than k, with no continuity assumed across the interface of the elements in $\mathcal{T}_h$, i.e.

$$V_h^k := \{v \in L^2(\Omega) : v|_K \in P^k(K), \quad \forall K \in \mathcal{T}_h\}. \tag{3.3}$$

P_h^l is the standard L^2 projection into V_h^l, $l \geq 0$ and we define $P_h^{-1} = P_h^0$. The damping coefficients σ_K^l are given as follows.

$$\sigma_K^l = \frac{2\,(2l+1)}{(2k-1)} \frac{h^l}{l!} \sum_{|\boldsymbol{\alpha}|=l} \left(\frac{1}{N_e} \sum_{\boldsymbol{v} \in K} \left([\![\partial^{\boldsymbol{\alpha}} u_h]\!] \big|_{\boldsymbol{v}} \right)^2 \right)^{\frac{1}{2}}, \quad k \geq 1, \tag{3.4}$$

where the vector $\boldsymbol{\alpha} = (\alpha_1, \ldots, \alpha_d)$ is the multi-index of order

$$|\boldsymbol{\alpha}| = \alpha_1 + \cdots + \alpha_d,$$

and $\partial^{\boldsymbol{\alpha}} w$ is defined as

$$\partial^{\boldsymbol{\alpha}} w = \frac{\partial^{|\boldsymbol{\alpha}|} w}{\partial x_1^{\alpha_1} \cdots \partial x_d^{\alpha_d}} = \partial_{x_1}^{\alpha_1} \cdots \partial_{x_d}^{\alpha_d} w.$$

N_e is the number of edges of the element K and $\boldsymbol{v} \in K$ are the vertices of K. $[\![w]\!]\big|_{\boldsymbol{v}}$ denotes the jump of the function w on the vertex $\boldsymbol{v}$. It should be noted that w may have several jumps on the vertex $\boldsymbol{v}$, and we only compute the jump between the element K and its adjacent neighbors. More specifically, we take the two-dimensional case as an illustration example in the following.

FIG. 3.1. *Graph for the illustration of the jumps in* σ_K^l *defined in* (3.4).

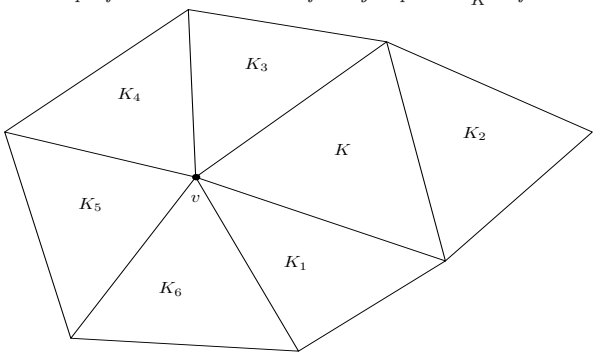

In Figure 3.1, we consider the jump of the function w on the vertex $\boldsymbol{v} \in K$. The element K has three edges thus $N_e = 3$. The adjacent neighbors of element K are K_1, K_2, K_3, then we define

$$\left([\![\partial^{\boldsymbol{\alpha}} w]\!] \big|_{\boldsymbol{v}} \right)^2 = \left[(w|_K - w|_{K_1})^2 + (w|_K - w|_{K_3})^2 \right] \Big|_{\boldsymbol{v}}.$$

Note that we do not take the elements K_4, K_5, K_6 into consideration, though we still have jumps between the element K and them on the vertex $\boldsymbol{v}$.

3.2. Conservation, L^2-boundedness and optimal error estimates.

3.2.1. Conservation. Take $v_h = 1$ in (3.2), we have

$$\begin{aligned}\frac{d}{dt}\int_K u_h\,d\boldsymbol{x} &= \int_{\partial K}\widehat{\boldsymbol{f}}(u_h)\cdot\boldsymbol{n}_K\,dS - \sum_{l=0}^{k}\frac{\sigma_K^l}{h_K}\int_K\left(u_h - P_h^{l-1}u_h\right)d\boldsymbol{x},\\ &= \int_{\partial K}\widehat{\boldsymbol{f}}(u_h)\cdot\boldsymbol{n}_K\,dS\,.\end{aligned}$$

Take summation over $K\in\mathcal{T}_h$, with the periodic or the compactly supported boundary conditions, and we obtain the following conservation result for the DG scheme (3.2).

$$\frac{d}{dt}\sum_{K\in\mathcal{T}_h}\int_K u_h\,d\boldsymbol{x} = 0.$$

3.2.2. L^2-boundedness. Taking $v_h = u_h$ in (3.2), we have

$$\begin{aligned}\frac{1}{2}\frac{d}{dt}\int_K u_h^2\,d\boldsymbol{x} &= \int_K \boldsymbol{f}(u_h)\cdot\nabla u_h\,d\boldsymbol{x}\\ &\quad+\int_{\partial K}\widehat{\boldsymbol{f}}(u_h)\cdot\boldsymbol{n}_K u_h\,dS - \sum_{l=0}^{k}\frac{\sigma_K^l}{h_K}\int_K\left(u_h - P_h^{l-1}u_h\right)^2 d\boldsymbol{x}\end{aligned}$$

Take summation over $K\in\mathcal{T}_h$, with the periodic or the compactly supported boundary conditions, and we obtain the L^2 stability result if the monotone numerical flux is used on the element interface.

$$\frac{d}{dt}\sum_{K\in\mathcal{T}_h}\int_K u_h^2\,d\boldsymbol{x}\le 0. \tag{3.5}$$

Then it indicates $\|u_h(\cdot,t)\|$ is bounded by $\|u_h(\cdot,0)\|$.

3.2.3. A priori error estimates. In the following we proceed to derive the a priori error estimates for the DG scheme (3.2). As is well known, for multidimensional Cartesian meshes, the optimal results are usually based on using Q^k-elements, namely the space of tensor-product polynomials of degree at most k in each variable. Recently, in [31] the authors developed a shifting technique to construct a special projection to obtain the optimal error estimates for the P^k space. We continue to use this technique to study the optimal error estimates for our DG method. Now we also consider the two-dimensional linear equation and assume that $\boldsymbol{f}(u) = (u,u)$ without loss of generality. Due to technical reasons, we study the error estimates on the uniform Cartesian meshes. Though we consider the two-dimensional problem in this section, the analysis can be extended to the higher dimensional cases $d > 2$ without any difficulties. We now have the following error estimation of the DG scheme (3.2) for two-dimensional linear hyperbolic conservation laws.

THEOREM 3.1. *For any given integer $k\ge 1$, suppose $u(\cdot,t)\in H^{k+2}(\Omega)$ is the exact solution of the problem* (3.1) *with the linear flux $\boldsymbol{f}(u) = (u,u)$ and u_h is the numerical solution of DG scheme* (3.2) *with uniform meshes. The initial data is chosen by $u_h(x,0) = P_h^k u_0$, where P_h^k is the standard L^2 projection, then we have*

$$\left\|u(\cdot,t) - u_h(\cdot,t)\right\| \lesssim h^{k+1}\,. \tag{3.6}$$

Before we proceed, we introduce some notations for convenience. Denote

$$K_{i,j} = I_i \times J_j, \quad I_i = \big(x_{i-\frac{1}{2}}, x_{i+\frac{1}{2}}\big),\ J_j = \big(y_{j-\frac{1}{2}}, y_{j+\frac{1}{2}}\big),\ i = 1, \ldots, N_x,\ j = 1, \ldots, N_y\,.$$

Let $h_x^i = x_{i+\frac{1}{2}} - x_{i-\frac{1}{2}}$, $h_y^j = y_{j+\frac{1}{2}} - y_{j-\frac{1}{2}}$. Since we have the assumption that the mesh is uniform in each direction, we denote $h_x = h_x^i$, $h_y = h_y^j$ and $h_{i,j} = \sqrt{h_x^2 + h_y^2}$, $\forall\, i, j$ and $h = \max(h_x, h_y)$. Similar to the one-dimensional case, we adopt the upwind numerical flux in the DG scheme (3.2). First we rewrite the DG scheme (3.2) into the following form.

$$\int_{K_{i,j}} (u_h)_t v_h \, dxdy + \widetilde{B}_{i,j}(u_h, v_h) + \sum_{l=0}^{k} \frac{\sigma_{K_{i,j}}^l}{h_{i,j}} \int_{K_{i,j}} \big(u_h - P_h^{l-1} u_h\big) v_h \, dxdy = 0\,, \tag{3.7}$$

where $\widetilde{B}_{i,j}(\cdot,\cdot)$ is given as

$$\begin{aligned} \widetilde{B}_{i,j}(w, v_h) = & -\int_{K_{i,j}} w\,(v_h)_x + w\,(v_h)_y \, dxdy \\ & + \int_{I_i} w\big(x, y^-_{j+\frac{1}{2}}\big) v_h\big(x, y^-_{j+\frac{1}{2}}\big) - w\big(x, y^-_{j-\frac{1}{2}}\big) v_h\big(x, y^+_{j-\frac{1}{2}}\big)\, dx \\ & + \int_{J_j} w\big(x^-_{i+\frac{1}{2}}, y\big) v_h\big(x^-_{i+\frac{1}{2}}, y\big) - w\big(x^-_{i-\frac{1}{2}}, y\big) v_h\big(x^+_{i-\frac{1}{2}}, y\big)\, dy. \end{aligned} \tag{3.8}$$

Since the exact solution u also satisfies

$$\int_{K_{i,j}} u_t v_h \, dxdy + \widetilde{B}_{i,j}(u, v_h) = 0, \quad \forall\, v_h \in V_h^k\,,$$

we then immediately obtain the error equation as follows.

$$\begin{aligned} & \int_{K_{i,j}} (u - u_h)_t v_h \, dxdy + \widetilde{B}_{i,j}(u - u_h, v_h) \\ & \quad - \sum_{l=0}^{k} \frac{\sigma_{K_{i,j}}^l}{h_{i,j}} \int_{K_{i,j}} \big(u_h - P_h^{l-1} u_h\big) v_h \, dxdy = 0\,, \quad \forall\, v_h \in V_h^k. \end{aligned} \tag{3.9}$$

Next, we introduce a special projection constructed in [31], which is crucial in the derivation of the error estimates. We denote the projection as $\mathbb{P}^\star$, and for each $K_{i,j}$, find $\mathbb{P}^\star w(x,y) \in P^k(K_{i,j})$ such that

$$\begin{cases} \displaystyle\int_{K_{i,j}} \mathbb{P}^\star w(x,y)\, dxdy = \int_{K_{i,j}} w(x,y)\, dxdy\,, \\ \widetilde{P_h}(\mathbb{P}^\star w, v_h)_{i,j} = \widetilde{P_h}(w, v_h)_{i,j}, \quad \forall\, v_h \in P^k(K_{i,j}), \end{cases} \tag{3.10}$$

where $\widetilde{P_h}(w, v_h)_{i,j}$ is defined as follows

$$\begin{aligned} \widetilde{P_h}(w, v_h)_{i,j} = & \int_{K_{i,j}} \Big(w\,(v_h)_x + w\,(v_h)_y\Big)\, dxdy \\ & - \int_{I_i} w\big(x, y^-_{j+\frac{1}{2}}\big)\Big(v_h\big(x, y^-_{j+\frac{1}{2}}\big) - v_h\big(x, y^+_{j-\frac{1}{2}}\big)\Big)\, dx \\ & - \int_{J_j} w\big(x^-_{i+\frac{1}{2}}, y\big)\Big(v_h\big(x^-_{i+\frac{1}{2}}, y\big) - v_h\big(x^+_{i-\frac{1}{2}}, y\big)\Big)\, dy. \end{aligned} \tag{3.11}$$

It has already been shown that the projection $\mathbb{P}^\star$ is well-defined in [31], and it also has the optimal approximation error estimates for a smooth function w as follows

$$\|w - \mathbb{P}^\star w\|_{L^2(K_{i,j})} \lesssim h^{k+1}\|w\|_{k+1,K_{i,j}}. \tag{3.12}$$

We now take

$$\xi = \mathbb{P}^\star u - u_h, \quad \eta = \mathbb{P}^\star u - u. \tag{3.13}$$

Then for the error equation (3.9), we take the summation over i, j and obtain

$$\begin{aligned}
&\sum_{i,j}\int_{K_{i,j}} \xi_t v_h \, dxdy + \sum_{i,j} \widetilde{B}_{i,j}(\xi, v_h) \\
&\quad + \sum_{i,j}\sum_{l=0}^{k} \frac{\sigma^l_{K_{i,j}}}{h_{i,j}} \int_{K_{i,j}} \big(\xi - P_h^{l-1}\xi\big) v_h \, dxdy = B_1(v_h) + B_2(v_h), \quad \forall\, v_h \in V_h^k\,,
\end{aligned} \tag{3.14}$$

where B_1 and B_2 are defined as

$$\begin{aligned}
B_1(v_h) &= \sum_{i,j}\int_{K_{i,j}} \eta_t v_h \, dxdy + \sum_{i,j} \widetilde{B}_{i,j}(\eta, v_h), \\
B_2(v_h) &= \sum_{i,j}\sum_{l=0}^{k} \frac{\sigma^l_{K_{i,j}}}{h_{i,j}} \int_{K_{i,j}} \big(\mathbb{P}^\star u - P_h^{l-1}(\mathbb{P}^\star u)\big) v_h \, dxdy\,.
\end{aligned}$$

For the left-hand side of (3.14), we take $v_h = \xi$ and use the stability result to obtain

$$\begin{aligned}
&\sum_{i,j}\int_{K_{i,j}} \xi_t \xi \, dxdy + \sum_{i,j} \widetilde{B}_{i,j}(\xi, \xi) + \sum_{i,j}\sum_{l=0}^{k} \frac{\sigma^l_{K_{i,j}}}{h_{i,j}} \int_{K_{i,j}} \big(\xi - P_h^{l-1}\xi\big)\xi \, dxdy \\
&\quad = \frac{1}{2}\frac{d}{dt}\|\xi\|^2 + \frac{1}{2}\sum_{i,j}\int_{J_j} \Big(\llbracket \xi \rrbracket\big(x_{i+\frac{1}{2}}, y\big)\Big)^2 dy + \frac{1}{2}\sum_{i,j}\int_{I_i} \Big(\llbracket \xi \rrbracket\big(x, y_{j+\frac{1}{2}}\big)\Big)^2 dx \\
&\qquad + \sum_{i,j}\sum_{l=0}^{k} \frac{\sigma^l_{K_{i,j}}}{h_{i,j}} \int_{K_{i,j}} \big(\xi - P_h^{l-1}\xi\big)^2 dxdy\,,
\end{aligned} \tag{3.15}$$

where $\llbracket \xi \rrbracket\big(x_{i+\frac{1}{2}}, y\big) = \xi\big(x^+_{i+\frac{1}{2}}, y\big) - \xi\big(x^-_{i+\frac{1}{2}}, y\big)$, $\llbracket \xi \rrbracket\big(x, y_{j+\frac{1}{2}}\big) = \xi\big(x, y^+_{j+\frac{1}{2}}\big) - \xi\big(x, y^-_{j+\frac{1}{2}}\big)$. In [31], we have

$$B_1(\xi) \lesssim h^{2k+2}\|u\|_{H^{k+2}(\Omega)} + \|\xi\|^2. \tag{3.16}$$

For $B_2(\xi)$, we have the fact that

$$\|\mathbb{P}^\star u - P_h^{l-1}(\mathbb{P}^\star u)\|_{L^2(K_{i,j})} \lesssim h^{\max(1,l-1)+1}, \quad l = 0, \ldots, k \tag{3.17}$$

and with the definition of $\sigma^l_{K_{i,j}}$ in (3.4), we have

$$\begin{aligned}
\sum_{i,j}\big(\sigma^l_{K_{i,j}}\big)^2 &= \sum_{i,j} \frac{4\,(2l+1)^2}{(2k-1)^2}\frac{h^{2l}}{(l!)^2} \sum_{|\boldsymbol{\alpha}|=l}\left(\frac{1}{N_e}\sum_{\boldsymbol{v}\in K_{i,j}} \Big(\llbracket \partial^{\boldsymbol{\alpha}} u_h - \partial^{\boldsymbol{\alpha}} u \rrbracket\big|_{\boldsymbol{v}}\Big)^2\right) \\
&\lesssim \sum_{i,j}\sum_{|\boldsymbol{\alpha}|=l} \frac{h^{2l}}{N_e} \sum_{\boldsymbol{v}\in K_{i,j}} \Big(\llbracket \partial^{\boldsymbol{\alpha}}\xi \rrbracket^2\big|_{\boldsymbol{v}} + \llbracket \partial^{\boldsymbol{\alpha}}\eta \rrbracket^2\big|_{\boldsymbol{v}}\Big) \lesssim h^{-2}\|\xi\|^2 + h^{2k}.
\end{aligned} \tag{3.18}$$

For the last inequality, we have used the inverse inequality, Theorem 3.2.6. in [14]. Therefore, by the Cauchy-Schwarz inequality we have

$$
\begin{aligned}
B_2(\xi) &\lesssim \sum_{i,j}\sum_{l=0}^{k}\frac{(\sigma^l_{K_{i,j}})^2}{h_K^2}\|\mathbb{P}^\star u - P_h^{l-1}(\mathbb{P}^\star u)\|^2_{L^2(K_{i,j})} + \|\xi\|^2 \\
&\lesssim \sum_{i,j}\sum_{l=0}^{k}\frac{(\sigma^l_{K_{i,j}})^2}{h_K^2}h^{2\max(l-1,1)+2} + \|\xi\|^2 \lesssim h^{2k+2} + \|\xi\|^2.
\end{aligned} \tag{3.19}
$$

Plug (3.15), (3.16) and (3.19) into (3.9), we then obtain

$$
\frac{1}{2}\frac{d}{dt}\|\xi\|^2 \lesssim h^{2k+2} + \|\xi\|^2. \tag{3.20}
$$

Again Grönwall's inequality (2.28), together with the initial discretization, gives us the desired optimal error estimates.

4. Numerical tests. In this section, we present some numerical results to validate our theoretical results in both one- and two-dimensions. We adopt the classic fourth order Runge-Kutta method as our time stepping method for most cases in this section unless otherwise indicated. The CFL condition is $\tau = O(h)$, where τ and h are temporal step size and spatial step size, respectively.

4.1. One-dimensional problems. In this subsection, we present the numerical examples of one-dimensional problems. For the linear scalar problems, we use the ninth order strong stability preserving (SSP) Runge-Kutta method. To see the convergence behavior of the DG method, we use the nonuniform mesh and it is 10% random perturbation of the uniform mesh. For the nonlinear scalar problems, we just use the uniform Cartesian mesh for convenience. In the plots, the solid line in black is the reference solution, and the numerical solution is shown with the red circles.

EXAMPLE 1. *Consider the linear scalar conservation laws that* $f(u) = u$ *in* (2.1). *We consider two initial conditions:*

(a) The smooth case: $u_0(x) = \sin(2\pi x)^2$, $x \in (0, 1)$.

(b) The non-smooth case:

$$
u_0(x) = \begin{cases} \sin(2\pi x), & 0.3 \le x \le 0.8, \\ \cos(2\pi x) - 0.5, & \text{otherwise.} \end{cases}
$$

For both cases, the domain is $(0, 1)$ *and the final time is* $T = 1.1$.

In Table 4.1, We show the errors and convergence orders of $\|u-u_h\|$, $\|u-u_h^c\|$, $\|\xi\|$ and $e_{u,c}, e_{u,f}, e_{u,p}$ defined in (2.41) in Example 1, where u_h^c is the numerical solution of the classic DG scheme (2.4). As the mesh refines, the error between u_h and u_h^c is close indicating that the damping term becomes smaller on refined mesh when the exact solution stays smooth. Also, we can see the convergence orders of $\|\xi\|$, $e_{u,c}, e_{u,f}, e_{u,p}$ coincide well with the theoretical results and $\|\xi\|$ is dominant in $\|u-u_h\|$ on the coarse mesh for short time simulation. In Figure 4.2, we show the numerical solution of the mesh $N = 256$. We can see the shock discontinuity is well captured and the shock transition becomes sharper as we increase the degree of polynomials k, and spurious oscillations are eliminated effectively.

EXAMPLE 2. *Consider the Burgers' equation that* $f(u) = u^2/2$ *in* (2.1). *The initial condition is* $u_0(x) = \sin(x) + 0.5$, $x \in (0, 2\pi)$. *We choose different final time*

TABLE 4.1
Errors and convergence orders of $\|u-u_h\|$, $\|u-u_h^c\|$, $\|\xi\|$, $e_{u,c}$, $e_{u,f}$, and $e_{u,p}$, with initial condition (a) in Example 1.

	N	$\|u-u_h\|$	order	$\|u-u_h^c\|$	order	$\|\xi\|$	order	$e_{u,c}$	order	$e_{u,f}$	order	$e_{u,p}$	order
P^1	16	1.482E-01	–	3.326E-02	–	1.478E-01	–	1.435E-01	–	1.486E-01	–	2.134E-01	–
	32	3.022E-02	2.258	5.291E-03	2.579	2.999E-02	2.523	2.961E-02	2.307	2.992E-02	2.492	5.005E-02	2.056
	64	4.950E-03	2.821	1.012E-03	2.479	4.864E-03	2.628	4.815E-03	2.665	4.852E-03	2.544	8.624E-03	2.528
	128	7.495E-04	2.632	2.233E-04	2.219	7.206E-04	2.808	7.153E-04	2.792	7.191E-04	2.776	1.177E-03	2.763
	256	1.100E-04	2.862	5.402E-05	1.997	9.590E-05	2.877	9.607E-05	2.939	9.617E-05	2.882	1.495E-04	3.107
	512	1.820E-05	2.602	1.344E-05	1.995	1.236E-05	3.012	1.235E-05	2.986	1.236E-05	3.057	1.875E-05	3.021
P^2	16	1.204E-02	–	9.244E-04	–	1.220E-02	–	1.173E-02	–	1.297E-02	–	1.621E-02	–
	32	7.979E-04	4.053	1.134E-04	3.063	7.847E-04	3.980	7.675E-04	3.892	7.939E-04	4.035	1.171E-03	3.971
	64	4.896E-05	4.045	1.422E-05	3.143	4.673E-05	4.162	4.747E-05	4.178	4.731E-05	3.973	6.854E-05	4.168
	128	3.374E-06	3.944	1.761E-06	2.953	2.801E-06	4.092	2.812E-06	4.118	2.812E-06	4.212	4.122E-06	4.091
	256	2.796E-07	3.564	2.188E-07	3.045	1.701E-07	4.070	1.701E-07	4.049	1.697E-07	3.949	2.536E-07	4.050
	512	2.953E-08	3.285	2.748E-08	3.021	1.055E-08	4.034	1.056E-08	4.055	1.057E-08	4.132	1.557E-08	4.001
P^3	16	7.309E-04	–	4.516E-05	–	7.253E-04	–	6.687E-04	–	7.022E-04	–	1.309E-03	–
	32	2.565E-05	4.875	2.842E-06	4.244	2.610E-05	5.195	2.435E-05	5.167	2.573E-05	4.922	4.396E-05	5.257
	64	9.014E-07	5.015	1.799E-07	4.046	8.812E-07	4.700	8.591E-07	4.767	8.783E-07	4.850	1.398E-06	5.063
	128	3.089E-08	4.805	1.086E-08	4.074	2.955E-08	5.073	2.917E-08	5.249	2.890E-08	4.921	4.314E-08	4.952
	256	1.148E-09	4.997	6.903E-10	4.031	9.375E-10	4.925	9.269E-10	4.868	9.323E-10	5.000	1.358E-09	4.990
	512	5.243E-11	4.472	4.313E-11	4.021	2.956E-11	5.065	2.940E-11	5.031	2.964E-11	4.993	4.291E-11	5.080

FIG. 4.2. *The numerical solution with the initial condition (b) in Example 1.*

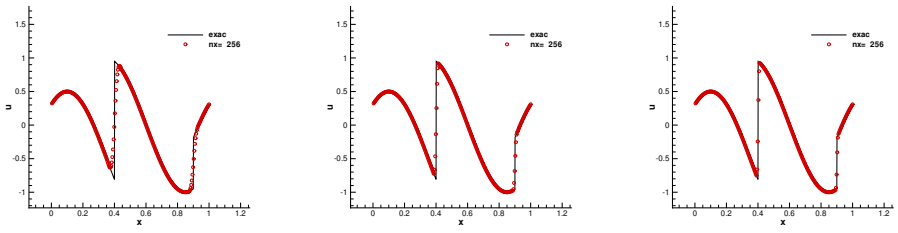

(a) P^1-element. (b) P^2-element. (c) P^3-element.

to test our algorithm. Note that when the final time $T = 0.6$, the exact solution is smooth. While if we choose the final time $T = 2.2$, then there is a shock developed inside the domain.

In Example 2, the exact solution of the one-dimensional Burgers' equation is smooth at time $T = 0.6$. We report the errors and convergence orders in Table 4.2, and we can see a very clean $(k+1)$-th order of convergence in L^1, L^2 and L^∞ norms. In Figure 4.3, we plot the numerical solution at time $T = 2.2$, when there is a shock inside the domain. We can see there are no spurious numerical oscillations near the discontinuity, which validates the good performance of our algorithm.

4.2. Two-dimensional problems. In this subsection, we present two-dimensional numerical examples, including the linear and nonlinear problems. For simplicity, we adopt uniform Cartesian meshes throughout this subsection.

EXAMPLE 3. *Consider the two-dimensional linear scalar conservation laws:*

$$u_t + u_x + u_y = 0, \quad (x, y) \in (-1, 1) \times (-1, 1)$$

with periodic boundary condition. We consider two initial conditions in the following.
(a) The smooth case: $u_0(x, y) = \sin(\pi(x + y))^2$.

TABLE 4.2
Errors and orders, and the final time $T = 0.6$ in Example 2.

	N	$\|u-u_h\|_{L^1}$	order	$\|u-u_h\|_{L^2}$	order	$\|u-u_h\|_{L^\infty}$	order
P^1	16	1.054E-02	–	1.682E-02	–	5.511E-02	–
	32	1.829E-03	2.527	3.122E-02	2.430	1.514E-02	1.864
	64	3.939E-04	2.215	7.287E-03	2.099	4.128E-03	1.875
	128	9.262E-05	2.088	1.739E-03	2.067	9.644E-03	2.098
	256	2.218E-05	2.062	4.270E-04	2.026	2.624E-04	1.878
	512	5.462E-06	2.022	1.068E-05	2.000	6.908E-05	1.926
P^2	16	1.119E-03	–	2.334E-03	–	1.080E-02	–
	32	1.644E-04	2.766	3.914E-04	2.576	2.881E-03	1.907
	64	2.240E-05	2.876	5.808E-05	2.753	4.800E-04	2.586
	128	2.992E-06	2.904	8.261E-06	2.814	7.832E-05	2.616
	256	4.005E-07	2.901	1.173E-06	2.816	1.198E-05	2.708
	512	5.375E-08	2.898	1.640E-07	2.839	1.712E-06	2.807
P^3	16	2.052E-04	–	5.975E-04	–	3.071E-03	–
	32	1.263E-05	4.023	4.454E-05	3.746	3.269E-04	3.231
	64	6.577E-07	4.263	2.573E-06	4.114	2.361E-05	3.792
	128	3.192E-08	4.365	1.237E-07	4.378	1.415E-06	4.060
	256	1.577E-09	4.339	7.992E-09	4.385	7.992E-08	4.146
	512	8.811E-11	4.162	3.097E-10	4.257	4.292E-09	4.219

FIG. 4.3. *The numerical solution with final time $T = 2.2$ in Example 2.*

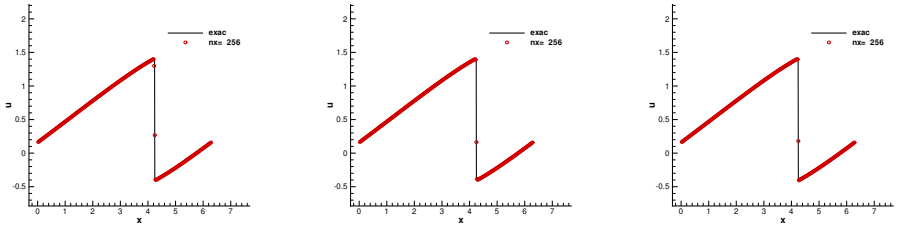

(a) P^1-element. (b) P^2-element. (c) P^3-element.

(b) The non-smooth case:

$$u_0(x,y) = \begin{cases} 1, & (x^2+y^2)^{\frac{1}{2}} \le \dfrac{1}{8}\left(3+3^{5\sin\theta}\right), \\ 0, & \text{elsewhere}, \end{cases}$$

where θ is given as

$$\theta = \arccos\frac{x}{\sqrt{x^2+y^2}}, \text{ when } y \ge 0, \text{ and } \theta = 2\pi - \arccos\frac{x}{\sqrt{x^2+y^2}}, \text{ when } y < 0.$$

We take the final time $T = 1.1$ for case (a) and $T = 1.8$ for case (b).

In Table 4.3, we show the errors and convergence orders in L^1, L^2 and L^∞ norms in Example 3. We can see the convergence orders are above $k+1$ for both P^1-element

and P^2-element. In Figure 4.4, we show the contours of the numerical solution and the cuts at $y = -1/4$ with initial condition (b). The spurious numerical oscillations are hardly seen in the figure and it implies the extra damping term does take effect.

TABLE 4.3
Errors and convergence orders, initial condition (a) in Example 3.

	$N_x \times N_y$	$\|u-u_h\|_{L^1}$	order	$\|u-u_h\|_{L^2}$	order	$\|u-u_h\|_{L^\infty}$	order
P^1	20×16	1.949E-01	–	2.171E-01	–	3.149E-01	–
	40×32	5.739E-02	1.764	6.646E-02	1.708	1.050E-01	1.585
	80×64	9.055E-03	2.664	1.144E-02	2.539	2.185E-02	2.265
	160×128	1.593E-03	2.507	1.838E-03	2.638	3.475E-03	2.653
	320×256	2.299E-04	2.792	2.641E-04	2.799	5.074E-04	2.776
P^2	20×16	6.761E-02	–	7.397E-02	–	1.021E-01	–
	40×32	5.936E-03	3.510	6.337E-03	3.545	1.098E-02	3.217
	80×64	3.846E-04	3.948	4.251E-04	3.898	9.146E-04	3.585
	160×128	2.382E-05	4.013	2.671E-05	3.992	8.023E-05	3.511
	320×256	1.521E-06	3.969	1.754E-06	3.929	8.050E-06	3.317

FIG. 4.4. *The numerical solution with the initial condition (b) in Example 3.*

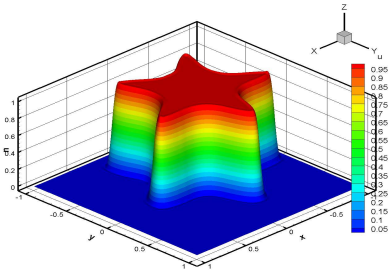

(a) P^1-element

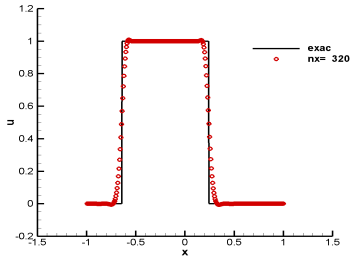

(b) The cut at $y = -1/4$ of (a)

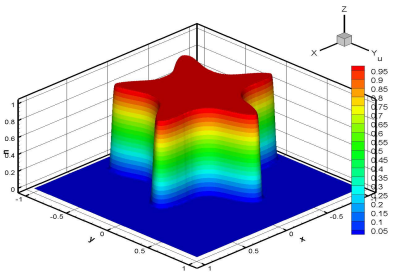

(c) P^2-element

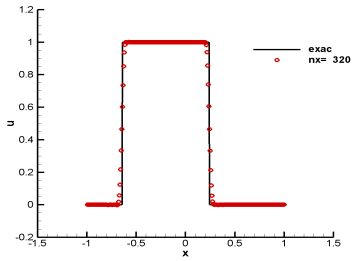

(d) The cut at $y = -1/4$ of (c)

EXAMPLE 4. *We consider two-dimensional Burgers' equation*

$$u_t + \left(\frac{u^2}{2}\right)_x + \left(\frac{u^2}{2}\right)_y = 0, \quad (x, y) \in \Omega.$$

We consider two cases in the following.

(a) The initial condition is $u_0(x,y) = \sin(\pi(x+y))$ *and periodic boundary condition. The computational domain is* $\Omega = (0, 2\pi) \times (0, 2\pi)$*, and we take the final time that* $T = 0.8$*.*

(b) Riemann problem [24] The computational domain is $\Omega = (0,1) \times (0,1)$ *and the final time is* $T = 0.5$*.*

In Figure 4.5, the shock is developed inside the domain and we can see the shock is well captured by the DG scheme and there are no spurious oscillations from the cut figures at $y = 3\pi/4$. In Figure 4.6, we plot the numerical solution for the Riemann problem. From the figures we can see no spurious oscillations near the discontinuity, and it again indicates that our algorithm is capable of treating spurious oscillations.

FIG. 4.5. *Plots of the numerical solution with initial condition (a) in Example 4.* $N_x = 320$, $N_y = 256$. *The final time is* $T = 0.8$.

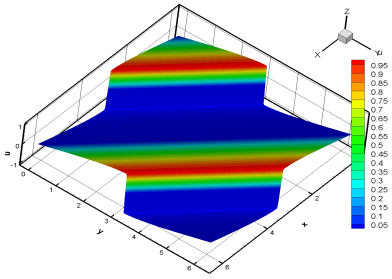

(a) P^1-element

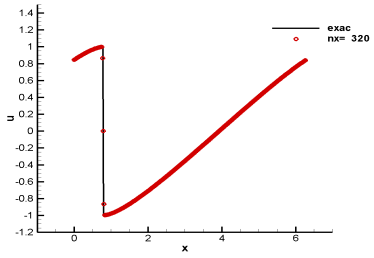

(b) The cut at $y = 3\pi/4$ of (a)

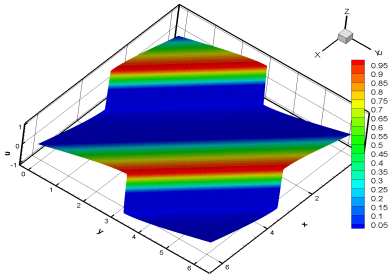

(c) P^2-element

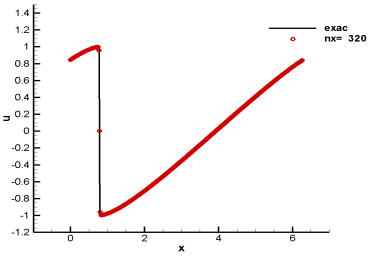

(d) The cut at $y = 3\pi/4$ of (c)

5. Concluding remarks. In this paper, we propose a new DG formulation for solving scalar hyperbolic conservation laws. Since the classic DG method would generate spurious oscillations that make the scheme less robust, our aim is to control spurious numerical oscillations near the discontinuities. By carefully introducing an extra damping term in the classic DG methods, we show that the new DG formulation still possesses many good properties such as conservation, L^2-boundedness, and optimal error estimates. In particular, for one-dimensional linear scalar conservation laws, with the correction function technique [11] we show the numerical solution still has the superconvergence behavior analogous to that of the classic DG schemes. In two-dimensional problems, we prove the optimal error estimates with P^k-elements by using the so-called shifting technique [31]. We provide several numerical examples in both linear and nonlinear, one- and two-dimensional cases, to show the robustness and effectiveness of the newly proposed DG method. Our next work is to extend the

FIG. 4.6. *Plots of the numerical solution with initial condition (b) in Example 4.* $N_x = 256$, $N_y = 256$. *The final time is* $T = 0.5$.

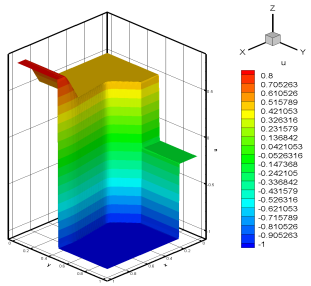

(a) P^1-element

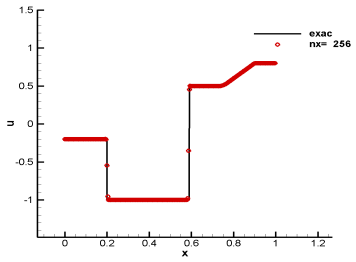

(b) The cut along the diagonal line (1,0) - (0,1) of (a)

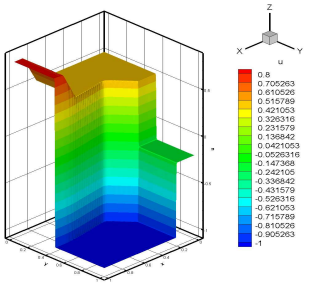

(c) P^2-element

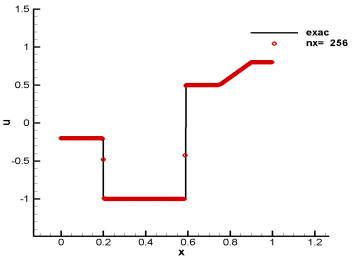

(d) The cut along the diagonal line (1,0) - (0,1) of (c)

current framework to systems, such as the inviscid compressible Euler equations. Besides, the choice of the damping term is obviously not unique and current definition has an influence on the convergence order for smooth problems on coarse meshes. Thus, to optimize the damping term so as to reduce its effect in the smooth region also constitutes our future work.

6. Appendix: Proofs of some lemmas and propositions. In this section, we give the proofs of some lemmas used in the paper.

6.1. Proof of Lemma 2.1. Since σ_j^l is not differentiable at $\left(\llbracket \partial_x^l u_h \rrbracket_{j+\frac{1}{2}}, \llbracket \partial_x^l u_h \rrbracket_{j-\frac{1}{2}}\right) = (0,0)$, we would like to proceed our proof by $(\sigma_\varepsilon)_j^l$ instead of σ_j^l that

$$(\sigma_\varepsilon)_j^l = \frac{2\,(2l+1)}{(2k-1)} \frac{h^l}{l!} \left(\llbracket \partial_x^l u_h \rrbracket_{j+\frac{1}{2}}^2 + \llbracket \partial_x^l u_h \rrbracket_{j-\frac{1}{2}}^2 + \varepsilon^2 \right)^{\frac{1}{2}}, \quad 0 < \varepsilon < h^{k+1}.$$

With this new $(\sigma_\varepsilon)_j^l$, we then take the derivative of the error equation (2.20) with respect to t and $\forall\, v_h \in V_h^k$ we have

$$\begin{aligned}
&\int_{I_j} \xi_{tt} v_h \, dx + B_j(\xi_t, v_h) + \sum_{l=0}^{k} \frac{(\sigma_\varepsilon)_j^l}{h_j} \int_{I_j} \big(\xi_t - P_h^{l-1}\xi_t\big) v_h \, dx \\
&= \int_{I_j} \eta_{tt} v_h \, dx + B_j(\eta_t, v_h) + \sum_{l=0}^{k} \frac{(\sigma_\varepsilon)_j^l}{h_j} \int_{I_j} \Big((P_h^- u)_t - P_h^{l-1}(P_h^- u)_t\Big) v_h \, dx \\
&\quad + \sum_{l=0}^{k} \frac{\big((\sigma_\varepsilon)_j^l\big)_t}{h_j} \Big(\int_{I_j} \big(\xi - P_h^{l-1}\xi\big) v_h \, dx + \int_{I_j} \Big(P_h^- u - P_h^{l-1}\big(P_h^- u\big)\Big) v_h \, dx \Big).
\end{aligned} \tag{6.1}$$

Taking $v_h = \xi_t$ in (6.1) and summing it over j, we obtain

$$\frac{1}{2}\frac{d}{dt}\int_a^b \xi_t^2 \, dx + \frac{1}{2}\sum_j [\![\xi_t]\!]_{j+\frac{1}{2}}^2 + \sum_j \sum_{l=0}^{k} \frac{(\sigma_\varepsilon)_j^l}{h_j} \int_{I_j} \big(\xi_t - P_h^{l-1}\xi_t\big)^2 \, dx = \sum_{s=1}^{4} \mathcal{A}_s \,, \tag{6.2}$$

where $\mathcal{A}_1, \mathcal{A}_2, \mathcal{A}_3, \mathcal{A}_4$ are given as

$$\mathcal{A}_1 = \sum_j \int_{I_j} \eta_{tt}\xi_t \, dx, \quad \mathcal{A}_2 = \sum_j \sum_{l=0}^{k} \frac{(\sigma_\varepsilon)_j^l}{h_j} \int_{I_j} \Big((P_h^- u)_t - P_h^{l-1}(P_h^- u)_t\Big)\xi_t \, dx,$$

$$\mathcal{A}_3 = -\sum_j \sum_{l=0}^{k} \frac{\big((\sigma_\varepsilon)_j^l\big)_t}{h_j} \int_{I_j} \big(\xi - P_h^{l-1}\xi\big)\xi_t \, dx,$$

$$\mathcal{A}_4 = \sum_j \sum_{l=0}^{k} \frac{\big((\sigma_\varepsilon)_j^l\big)_t}{h_j} \int_{I_j} \Big(P_h^- u - P_h^{l-1}\big(P_h^- u\big)\Big)\xi_t \, dx \,.$$

For $\mathcal{A}_1$, we immediately have

$$\mathcal{A}_1 \lesssim h^{k+1}\|\xi_t\| \,. \tag{6.3}$$

For $\mathcal{A}_2$, on I_j we have

$$\begin{aligned}
&\big\|(P_h^- u)_t - P_h^{l-1}(P_h^- u)_t\big\|_{L^2(I_j)} \\
&\le \big\|P_h^- u_t - u_t\big\|_{L^2(I_j)} + \big\|u_t - P_h^{l-1}u_t\big\|_{L^2(I_j)} + \big\|P_h^{l-1}(u_t - P_h^- u_t)\big\|_{L^2(I_j)} \\
&\lesssim h^{\max(1,l)+\frac{1}{2}}, \quad l = 1, \ldots, k.
\end{aligned}$$

Then with the estimate of σ_j^l in (2.24), we can obtain

$$\mathcal{A}_2 \le \sum_j \sum_{l=0}^{k} \frac{(\sigma_\varepsilon)_j^l}{h_j} \big\|(P_h^- u)_t - P_h^{l-1}(P_h^- u)_t\big\|_{L^2(I_j)} \|\xi_t\|_{L^2(I_j)} \lesssim (h^{k+1} + \varepsilon)\|\xi_t\| \,. \tag{6.4}$$

For $\mathcal{A}_3$, we should estimate $\big((\sigma_\varepsilon)_j^l\big)_t$ firstly. In fact, we have

$$\begin{aligned}
\big((\sigma_\varepsilon)_j^l\big)_t &= \big((\sigma_\varepsilon)_j^l\big)^{-1} \frac{2\,(2l+1)^2}{(2k-1)^2} \Big(\frac{h^l}{l!}\Big)^2 \Big(\big([\![\partial_x^l u_h]\!]_{j+\frac{1}{2}}^2\big)_t + \big([\![\partial_x^l u_h]\!]_{j-\frac{1}{2}}^2\big)_t \Big) \\
&\le \frac{2\,(2l+1)}{2k-1} \frac{h^l}{l!} \Big([\![\partial_x^l (u_h - u)_t]\!]_{j+\frac{1}{2}}^2 + [\![\partial_x^l (u_h - u)_t]\!]_{j-\frac{1}{2}}^2 \Big)^{\frac{1}{2}} \\
&\lesssim h^l \Big([\![\partial_x^l \xi_t]\!]_{j+\frac{1}{2}}^2 + [\![\partial_x^l \xi_t]\!]_{j-\frac{1}{2}}^2 \Big)^{\frac{1}{2}} + h^l \Big([\![\partial_x^l \eta_t]\!]_{j+\frac{1}{2}}^2 + [\![\partial_x^l \eta_t]\!]_{j-\frac{1}{2}}^2 \Big)^{\frac{1}{2}} .
\end{aligned} \tag{6.5}$$

Note that for $0<\varepsilon<h^{k+1}$ we still have $\|\xi(\cdot,t)\|\lesssim h^{k+1}$. Then we have the following estimate for $\mathcal{A}_3$.

$$
\begin{aligned}
\mathcal{A}_3 \lesssim & \sum_j \frac{1}{h_j}\sum_{l=0}^{k} h^l\Big(\llbracket\partial_x^l\xi_t\rrbracket_{j+\frac12}^2+\llbracket\partial_x^l\xi_t\rrbracket_{j-\frac12}^2\Big)^{\frac12}\big\|\xi-P_h^{l-1}\xi\big\|_{L^2(I_j)}\|\xi_t\|_{L^2(I_j)}\\
&+\sum_j \frac{1}{h_j}\sum_{l=0}^{k} h^l\Big(\llbracket\partial_x^l\eta_t\rrbracket_{j+\frac12}^2+\llbracket\partial_x^l\eta_t\rrbracket_{j-\frac12}^2\Big)^{\frac12}\big\|\xi-P_h^{l-1}\xi\big\|_{L^2(I_j)}\|\xi_t\|_{L^2(I_j)}\\
\lesssim & h^k\sum_j\sum_{l=0}^{k} h^l\Big(\llbracket\partial_x^l\xi_t\rrbracket_{j+\frac12}^2+\llbracket\partial_x^l\xi_t\rrbracket_{j-\frac12}^2\Big)^{\frac12}\|\xi_t\|_{L^2(I_j)}\\
&+h^k\sum_j\sum_{l=0}^{k} h^l\Big(\llbracket\partial_x^l\eta_t\rrbracket_{j+\frac12}^2+\llbracket\partial_x^l\eta_t\rrbracket_{j-\frac12}^2\Big)^{\frac12}\|\xi_t\|_{L^2(I_j)}\\
\lesssim & h^{k-\frac12}\|\xi_t\|^2+h^{2k+\frac12}\|\xi_t\|\,.
\end{aligned}
\tag{6.6}
$$

For $\mathcal{A}_4$, we have $\big\|P_h^-u-P_h^{l-1}(P_h^-u)\big\|_{L^2(I_j)}\lesssim h^{\max(l+\frac12,\frac32)}$, then with (6.5) we have

$$
\mathcal{A}_4\lesssim\|\xi_t\|^2+h^{k+1}\|\xi_t\|\,. \tag{6.7}
$$

Plug (6.3), (6.4), (6.6) and (6.7) into (6.2), then we obtain

$$
\begin{aligned}
&\frac12\frac{d}{dt}\int_a^b\xi_t^2\,dx+\frac12\sum_j\llbracket\xi_t\rrbracket_{j+\frac12}^2+\sum_j\sum_{l=0}^{k}\frac{(\sigma_\varepsilon)_j^l}{h_j}\int_{I_j}\big(\xi_t-P_h^{l-1}\xi_t\big)^2\,dx\\
&\quad\lesssim\|\xi_t\|^2+(h^{k+1}+\varepsilon)\|\xi_t\|\,.
\end{aligned}
\tag{6.8}
$$

With the Gronwall's inequality, we obtain

$$
\|\xi_t(\cdot,t)\|^2\lesssim\|\xi_t(\cdot,0)\|^2+(h^{k+1}+\varepsilon)^2\,. \tag{6.9}
$$

Let $\varepsilon\to0^+$ in (6.9), then the result still holds true. To bound $\|\xi_t(\cdot,0)\|$, we take the initial condition $u_h(x,0)=P_h^-u_0$ such that $\xi(x,0)=0$, $\forall\,x\in[a,b]$ and we take $t=0$ in the error equation (2.20), then $\forall\,v_h\in V_h^k$ we have

$$
\begin{aligned}
\int_{I_j}\xi_t(x,0)v_h\,dx=&\int_{I_j}\eta_t(x,0)v_h\,dx\\
&+\sum_{l=0}^{k}\frac{\sigma_j^l}{h_j}\int_{I_j}\Big(P_h^-u_0-P_h^{l-1}\big(P_h^-u_0\big)\Big)v_h\,dx\,.
\end{aligned}
\tag{6.10}
$$

Take $v_h=\xi_t(x,0)$ in (6.10) and sum it over j, we then obtain

$$
\begin{aligned}
\int_a^b\xi_t(x,0)^2\,dx=&\int_a^b\eta_t(x,0)\xi_t(x,0)\,dx\\
&+\sum_j\sum_{l=0}^{k}\frac{\sigma_j^l}{h_j}\Big(P_h^-u_0-P_h^{l-1}\big(P_h^-u_0\big)\Big)\xi_t(x,0)\,dx\,.
\end{aligned}
\tag{6.11}
$$

Similar to the estimates for A_1 and A_2 in (2.22) and (2.25), we can obtain

$$
\int_a^b\eta_t(x,0)\xi_t(x,0)\,dx\lesssim h^{k+1}\|\xi_t(\cdot,0)\|\,,
$$

$$\sum_j \sum_{l=0}^{k} \frac{\sigma_j^l}{h_j} \int_{I_j} \left(P_h^- u_0 - P_h^{l-1}\left(P_h^- u_0\right)\right) \xi_t(x,0)\, dx \lesssim h^{k+1} \left\| \xi_t(\cdot,0) \right\| .$$

Plug the above estimates into (6.11), then we obtain $\|\xi_t(\cdot,0)\| \lesssim h^{k+1}$. Therefore, we obtain the desired result (2.30). □

6.2. Proof of Lemma 2.2. Since $w \in P^k(I_j)$, we assume w has the following expression

$$w(x)\big|_{I_j} = \sum_{l=0}^{k} w_l L_{l,j}(x) , \tag{6.12}$$

where $L_{l,j}(x)$ is the standard Legendre polynomial of degree l in the interval I_j. Now we take test function v_h in first equation in (2.33) as follows.

$$v_h(x) = D^{-1} L_{l,j}(x) = \int_{x_{j-\frac{1}{2}}}^{x} L_{l,j}(s)\, ds, \quad l = 0, \ldots, k-1 .$$

Then we have

$$|w_l| \lesssim h^{\frac{1}{2}} \|\eta_t\|_{L^2(I_j)} + h \left(\sum_{l=0}^{k} \left|\sigma_j^l\right| \right), \quad l = 0, \ldots, k-1 , \tag{6.13}$$

where we have already used the estimation (2.34). Since $w^-_{j+\frac{1}{2}} = 0$, we have

$$|w_k| \lesssim \sum_{l=0}^{k-1} |w_l| \lesssim h^{\frac{1}{2}} \|\eta_t\|_{L^2(I_j)} + h \left(\sum_{l=0}^{k} \left|\sigma_j^l\right| \right) . \tag{6.14}$$

Thus we obtain

$$\|w\|_{L^(I_j)} \lesssim h^{\frac{1}{2}} \left(\sum_{l=0}^{k} |w_l|^2 \right)^{\frac{1}{2}} \lesssim h \|\eta_t\|_{L^2(I_j)} + h^{\frac{3}{2}} \left(\sum_{l=0}^{k} \left|\sigma_j^l\right|^2 \right)^{\frac{1}{2}} . \tag{6.15}$$

From the estimation for w, we can see the correction w is well defined and we can take time derivative in (2.33). By the similar argument as before, we can obtain the estimation for w_t. □

6.3. Proof of Corollary 2.1. From (2.41), since $(u - P_h^- u)\big|_{I_j} \perp P^0(I_j)$, $(P_h^- u)^-_{j+\frac{1}{2}} = u_{j+\frac{1}{2}}$ and by using Cauchy-Schwarz inequality we have

$$e_{u,c} = \left(\frac{1}{N} \sum_j \left(\frac{1}{h_j} \int_{I_j} (P_h^- u - u_h)\, dx \right)^2 \right)^{\frac{1}{2}} \le \|\xi\| \lesssim h^{k+2} ,$$

$$e_{u,f} = \left(\frac{1}{N} \sum_j \left((P_h^- u)^-_{j+\frac{1}{2}} - (u_h)^-_{j+\frac{1}{2}} \right)^2 \right)^{\frac{1}{2}} \lesssim \left(\frac{1}{N} \sum_j h^{-1} \|\xi\|^2_{I_j} \right)^{\frac{1}{2}} = \|\xi\| \lesssim h^{k+2}.$$

By the standard approximation theory,

$$\left| (u - P_h^- u)(G_{j,\ell}, t) \right| \lesssim h^{k+2} .$$

Therefore, we have

$$\begin{aligned} \left| (u - u_h)(G_{j,\ell}, t) \right| &\le \left| (u - P_h^- u)(G_{j,\ell}, t) \right| + \left| (P_h^- u - u_h)(G_{j,\ell}, t) \right| \\ &\lesssim h^{k+2} + h^{-\frac{1}{2}} \|\xi\| \lesssim h^{k+\frac{3}{2}} . \quad \square \end{aligned}$$

REFERENCES

[1] H. Atkins, B. Helenbrook, *Super-convergence of discontinuous Galerkin method applied to the Navier-Stokes equations*, 19th AIAA Computational Fluid Dynamics Conference, 2009.

[2] R. Becker, and M. Braack, *A two-level stabilization scheme for the Navier-Stokes equations*, Numerical Mathematics and Advanced Applications, 123 – 130, Springer, Berlin, 2004.

[3] M. Braack, and E. Burman, *Local projection stabilization for the Oseen problem and its interpretation as a variational multiscale method*, SIAM J. Numer. Anal. 43 (2006), 2544 – 2566.

[4] F. Brezzi, R.S. Falk, and L.D. Marini, *Basic principles of mixed virtual element methods*, ESAIM Math. Model. Numer. Anal. 48 (2014), 1227 – 1240.

[5] F. Bassi, and S. Rebay, *A high-order accurate discontinuous finite element method for the numerical solution of the compressible Navier-Stokes equations*, J. Comput. Phys. 131 (1997), 267 – 279.

[6] W. Cao, and Q. Huang, *Superconvergence of local discontinuous Galerkin methods for partial differential equations with higher order derivatives*, J. Sci. Comput. 72 (2017), 761 – 791.

[7] W. Cao, D. Li, Y. Yang, and Z. Zhang, *Superconvergence of discontinuous Galerkin methods based on upwind-biased fluxes for 1D linear hyperbolic equations*, ESAIM Math. Model. Numer. Anal. 51 (2017), 467 – 486.

[8] W. Cao, H. Liu, and Z. Zhang, *Superconvergence of the direct discontinuous Galerkin method for convection- diffusion equations*, Numer. Methods Partial Differential Equations 33 (2017), 290 – 317.

[9] W. Cao, C.-W. Shu, and Z. Zhang, *Superconvergence of discontinuous Galerkin methods for 1-D linear hyperbolic equations with degenerate variable coefficients*, ESAIM Math. Model. Numer. Anal. 51 (2017), 2213 – 2235.

[10] W. Cao, C.-W. Shu, Y. Yang, and Z. Zhang, *Superconvergence of discontinuous Galerkin method for nonlinear hyperbolic equations*, SIAM J. Numer. Anal. 56 (2018), 732 – 765.

[11] W. Cao, Z. Zhang, and Q. Zou, *Superconvergence of discontinuous Galerkin methods for linear hyperbolic equations*, SIAM J. Numer. Anal. 52 (2014), 2555 – 2573.

[12] Y. Cheng, and C.-W. Shu, *A discontinuous Galerkin finite element method for time dependent partial differential equations with higher order derivatives*, Math. Comp. 77 (2008), 699 – 730.

[13] Y. Cheng, and C.-W. Shu, *Superconvergence of discontinuous Galerkin and local discontinuous Galerkin schemes for linear hyperbolic and convection-diffusion equations in one space dimension*, SIAM J. Numer. Anal. 47 (2010), 4044 – 4072.

[14] P.G. Ciarlet, *The Finite Element Method for Elliptic Problems*, North Holland, Amsterdam, New York, 1978.

[15] B. Cockburn, S. Hou, and C.-W. Shu, *TVB Runge-Kutta local projection discontinuous Galerkin finite element method for conservation laws IV: The multidimensional case*, Math. Comp. 54 (1990), 545 – 581.

[16] B. Cockburn, G.E. Karniadakis, and C.-W. Shu, *The development of discontinuous Galerkin methods. Discontinuous Galerkin methods*, 3 – 50, Lect. Notes Comput. Sci. Eng. 11, Springer, Berlin, 2000.

[17] B. Cockburn, S.-Y. Lin, and C.-W. Shu, *TVB Runge-Kutta local projection discontinuous Galerkin finite element method for conservation laws III: One dimensional systems*, J. Comput. Phys. 84 (1989), 90 – 113.

[18] B. Cockburn, and C.-W. Shu, *The Runge-Kutta local projection P^1-discontinuous-Galerkin finite element method for scalar conservation laws*, ESAIM Math. Model. Numer. Anal. 25 (1991), 337 – 361.

[19] B. Cockburn, and C.-W. Shu, *TVB Runge-Kutta local projection discontinuous Galerkin finite element method for scalar conservation laws II: General framework*, Math. Comp. 52 (1989), 411 – 435.

[20] B. Cockburn, and C.-W. Shu, *The Runge-Kutta discontinuous Galerkin finite element method for conservation laws V: Multidimensional systems*, J. Comput. Phys. 141 (1998), 199 – 224.

[21] B. Cockburn, and C.-W. Shu, *The local discontinuous Galerkin method for time-dependent convection-diffusion systems*, SIAM J. Numer. Anal. 35 (1998), 2440 – 2463.

[22] P. Colella, and P.R. Woodward, *The piecewise parabolic method (PPM) for gas-dynamical simulations* J. Comput. Phys. 54 (1984), 174 – 201.

[23] S.K. Godunov, *A difference method for numerical calculation of discontinuous solutions of the equations of hydrodynamics*, (Russian) Mat. Sb. (N.S.) 47 (1959), 271 – 306.

[24] J.L. Guermond, R. Pasquetti, and B. Popov, *Entropy viscosity method for nonlinear conser-*

vation laws , J. Comput. Phys. 230 (2011), 4248 – 4267.
[25] A. Harten, *High resolution schemes for hyperbolic conservation laws*, J. Comput. Phys. 49 (1983), 357 – 393.
[26] A. Harten, B. Engquist, S. Osher, and S.R. Chakravarthy, *Uniformly high-order accurate essentially nonoscillatory schemes. III* , J. Comput. Phys. 71 (1987), 231 – 303.
[27] A. Hiltebrand, and S. Mishra, *Entropy stable shock capturing space time discontinuous Galerkin schemes for systems of conservation laws*, Numer. Math. 126 (2014), 103 – 151.
[28] G.-S. Jiang, and C.-W. Shu, *Efficient implementation of weighted ENO schemes*, J. Comput. Phys. 126 (1996), 202 – 228.
[29] L. Krivodonova, J. Xin, J.F. Remacle, N. Chevaugeon, and J.E. Flaherty, *Shock detection and limiting with discontinuous Galerkin methods for hyperbolic conservation laws*, Appl. Numer. Math. 48 (2004), 323 – 338.
[30] Y. Liu, C.-W. Shu, and M. Zhang, *Superconvergence of energy-conserving discontinuous Galerkin methods for linear hyperbolic equations*, Comm. Appl. Math. Comp. 1 (2019), 101–116.
[31] Y. Liu, C.-W. Shu, and M. Zhang, *Optimal error estimates of the semidiscrete discontinuous Galerkin methods for two dimensional hyperbolic equations on Cartesian meshes using P^k elements*, ESAIM Math. Model. Numer. Anal. 54 (2020), 705 – 726.
[32] Y. Liu, Q. Tao, and C.-W. Shu, *Analysis of optimal superconvergence of an ultraweak-local discontinuous Galerkin method for a time dependent fourth-order equation*, ESAIM Math. Model. Numer. Anal. 54 (2020), 1797 – 1820.
[33] J.-X. Qiu, and C.-W. Shu, *Runge-Kutta discontinuous Galerkin method using WENO limiters*, SIAM J. Sci. Comput. 26 (2005), 907 – 929.
[34] W.H. Reed and T.R. Hill, *Triangular mesh methods for the neutron transport equation*, Los Alamos Scientific Laboratory report LA-UR-73-479, NM, 1973.
[35] C.-W. Shu, *Discontinuous Galerkin methods: General approach and stability. Numerical solutions of partial differential equations*, 149 – 201, Adv. Courses Math. CRM Barcelona, Birkhäuser, Basel, 2009.
[36] C.-W. Shu, *Discontinuous Galerkin methods for time-dependent convection dominated problems: basics, recent developments and comparison with other methods. Building bridges: connections and challenges in modern approaches to numerical partial differential equations*, 369 – 397, Lect. Notes Comput. Sci. Eng. 114, Springer, 2016.
[37] C.-W. Shu, and S. Osher, *Efficient implementation of essentially nonoscillatory shock-capturing schemes*, J. Comput. Phys. 77 (1988), 439 – 471.
[38] B. van Leer, *Towards the ultimate conservative difference scheme V. A second-order sequel to Godunov's method*, J. Comput. Phys. 32 (1979), 101 – 136.
[39] P.E. Vincent, P. Castonguay and A. Jameson, *Insights from von Neumann analysis of high-order flux reconstruction schemes*, J. Comput. Phys. 230 (2011), 8134 – 8154.
[40] Y. Xu, and C.-W. Shu, *Local discontinuous Galerkin methods for high-order time-dependent partial differential equations*, Commun. Comput. Phys. 7 (2010), 1 – 46.
[41] J. Yan, and C.-W. Shu, *Local discontinuous Galerkin methods for partial differential equations with higher order derivatives*, J. Sci. Comput. 17 (2002), 27 – 47.
[42] Y. Yang and C.-W. Shu, *Analysis of optimal superconvergence of discontinuous Galerkin method for linear hyperbolic equations*, SIAM J. Numer. Anal. 50 (2012), 3110 – 3133.
[43] X. Zhang, and C.-W. Shu, *On maximum-principle-satisfying high order schemes for scalar conservation laws*, J. Comput. Phys. (229) 2010, 3091 – 3120.
[44] X. Zhong, and C.-W. Shu, *A simple weighted essentially nonoscillatory limiter for Runge-Kutta discontinuous Galerkin methods*, J. Comput. Phys. 232 (2013), 397 – 415.